Supporting Information for:

On the Syneresis of an OPV Functionalised Dipeptide Hydrogel

Ana M. Castilla,[a] Matthew Wallace,[a] Laura L. E. Mears,[a] Emily R. Draper,[a] James Doutch,[b] Sarah Rogers[b] and Dave J. Adams[a,*]

[a]Department of Chemistry, University of Liverpool, Crown Street, Liverpool, L69 7ZD, United Kingdom. E-mail: d.j.adams@liverpool.ac.uk

[b]ISIS Pulse Neutron Source, Rutherford Appleton Laboratory, Didcot, UK.

Table of Contents

1. Synthesis and characterisation

General Methods.

Solvents and reagents were purchased from commercial sources and used without further purification unless specified otherwise. *N*-Methyl-2-pyrrolidone (NMP) and dichloromethane (DCM) were purchased from Sigma-Aldrich as anhydrous solvents. 4,4'-((1*E*,1'*E*)-1,4-Phenylenebis(ethene-2,1-diyl))dibenzoic acid (**OPV-3 diacid**) was prepared following literature methods.[S1]

NMR spectroscopy

NMR spectra were recorded at 298 K using a Bruker Avance VIII HD 500 MHz spectrometer; Chemical shifts for ^{1}H and ^{13}C are reported in parts per million (δ); δ_H values are referenced to the residual solvent signal of $(CD_3)_2SO$ at δ = 2.50, and δ_C values are referenced to the solvent signal of $(CD_3)_2SO$ at δ = 39.52. NMR signals are reported in terms of chemical shifts (δ) in ppm, multiplicity, coupling constant (*J*) in Hertz (Hz), relative integral and assignment, in that order. The following abbreviations are used in reporting the multiplicity for NMR resonances: s = singlet, d = doublet, t = triplet, dd = doublet of doublets, qu = quartet, qn = quintet, sex = sextet, m = multiplet and br = broad signal. Spectra were processed using Bruker Topspin 3.2 (licensed to the Department of Chemistry, the University of Liverpool). Assignment of all ^{1}H and ^{13}C resonances was achieved using standard 2D NMR techniques such as ^{1}H-^{1}H COSY and ^{1}H-^{13}C HSQC.

Mass spectrometry

Measurements were carried out using a Waters Micromass Electrospray LCT Mass Spectrometer in positive or negative mode. Samples were run by the University of Liverpool mass spectrometry service.

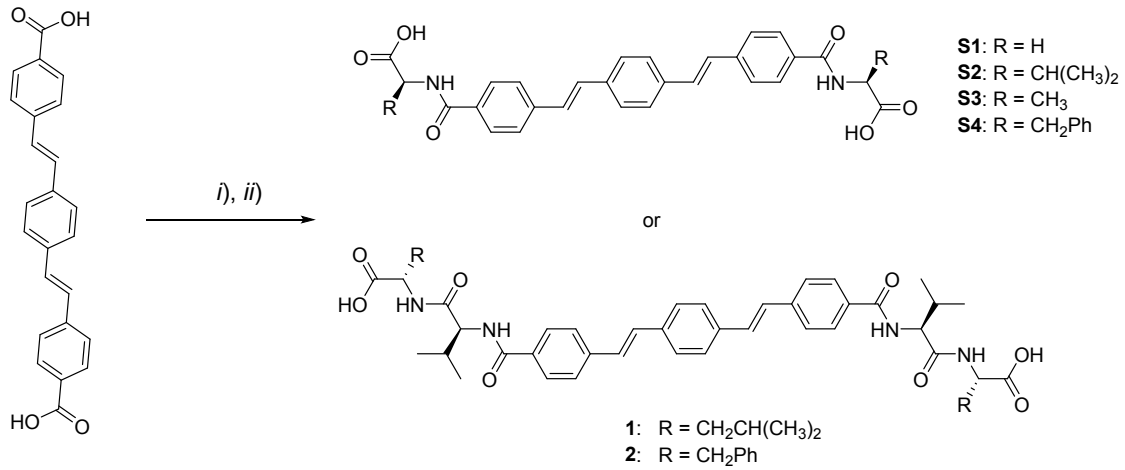

Scheme S1. **Reagents and conditions:** *i*) $SOCl_2$, then TFA.H_3N-L-Val-L-Leu/Phe-OMe or L-Gly/Val/Ala/Phe-OMe.HCl, Et_3N, DCM/NMP. *ii*) LiOH, THF/H_2O 3:1, r.t.

Synthesis of L-valyl-L-leucine methyl ester trifluoroacetate salt. Isobutyl chloroformate (5.2 mL, 40 mmol) was added to a solution of *N*-Boc-L-valine (8.7 gr, 40 mmol) and *N*-methylmorpholine (NMM, 4.4 mL, 40 mmol) in chloroform (100 mL) at -10 °C (ice-bath with added ammonium chloride). After stirring 5 -10 min, a solution of L-leucine methyl ester hydrochloride (7.3 gr, 40mmol) and NMM (4.4 mL, 40 mmol) in chloroform (50 mL) was added. The mixture was allowed to warm to room temperature and stirred overnight. The day after the organic solution was washed with water (2×), 0.2 M HCl, 0.2 M Na_2CO_3 and brine. After drying over sodium sulphate the solvent was evaporated under reduced pressure. The white powder obtained was then dissolved in a mixture of chloroform (15mL) and trifluoroacetic acid (15 mL) and the mixture stirred overnight at room temperature. Addition of diethyl ether to the reaction mixture induced precipitation. The solid was collected and washed with diethyl ether (13 gr, 95%). All spectroscopic data matched those in literature.[S2]

Synthesis of L-valyl-L-phenylalanine methyl ester trifluoroacetate salt. The procedure described above was followed starting from *N*-Boc-L-valine (8.7 gr, 40 mmol) and L-phenylalanine methyl ester hydrochloride (8.7 gr, 40 mmol). The product was obtained as a white solid (12.5 gr, 80%). All spectroscopic data matched those in literature.[S3]

Synthesis of LMWG 1: **OPV-3 diacid** (631 mg, 1.7 mmol) was suspended in thionyl chloride (15 mL), added 2 drops of DMF and refluxed until the solid was completely dissolved (aprox. 16 h). A mixture of anhydrous DCM/NMP 2:1 (20 mL) and DMAP (catalytic amount) were added to the solid

residue and stirred for 10 min. The mixture was cooled down to 0 ºC and a solution of L-valyl-L-leucine methyl ester trifluoroacetate salt (1.34 gr, 3.7 mmol) and triethylamine (1.3 mL, 9.3 mmol) in dry DCM (5 mL) were added dropwise. The resulting mixture was allowed to stir overnight at room temperature under N_2. The day after the DCM was evaporated under reduced pressure and water added to the resulting dark liquid residue. The solid formed was collected by filtration, washed thoroughly with water and dried under vacuum. The dried solid was then triturated with acid water, collected again by filtration and washed with water, methanol, dichloromethane, and dried under vacuum for 24 h to obtain the methyl protected gelator **1** as a dark yellow solid (1.3 gr, 93%). The product can be further purified by dissolving it in hot DCM, filtering while still hot and adding diethyl ether to the filtrate to precipitate the pure product out. A sample of this solid (820 mg, 1.0 mmol) was suspended in THF/H_2O 3:1 (25 mL) and LiOH (0.35 gr) added. The resulting mixture was stirred overnight at room temperature. The day after the mixture was acidified with HCl 2M until pH ~ 3. The solid obtained was collected by filtration, thoroughly washed with water and dried under vacuum. Gelator **1** was obtained as a pale yellow solid (786 mg, 99% second step, 92% overall yield). ^{1}H NMR (DMSO, 500 MHz): δ = 12.49 (br, 1H), 8.22 (d, *J* = 9.6 Hz, 2H), 7.90 (d, *J* = 9.0 Hz, 2H), 7.71 (d, *J* = 8.3 Hz, 2H), 7.68 (s, 2H), 7.42 (d, *J* = 16.5 Hz, 1H), 7.37 (d, *J* = 16.4 Hz, 1H), 4.36 (t, *J* = 8.4 Hz, 1H), 4.24 (m, 1H), 2.13 (m, 1H), 1.67 (m, 1H), 1.55 (m, 2H), 0.97 (d, *J* = 6.7 Hz, 3H), 0.94 (d, *J* = 6.7 Hz, 3H), 0.91 (d, *J* = 6.5 Hz, 3H), 0.84 (d, *J* = 6.7 Hz, 3H); ^{13}C (DMSO, 125 MHz): δ = 174.4, 171.7, 166.4, 140.4, 136.9, 133.5, 130.2, 128.5(2C), 128.1, 127.6(2C), 126.7(2C), 59.2, 50.7, 40.4 (overlapping with the solving signal), 30.8, 24.7, 23.3, 21.8, 19.7, 19.3. HRMS (ESI-MS): *m*/*z* $[M + Na]^+$ (calcd. 817.4152): found 817.4131.

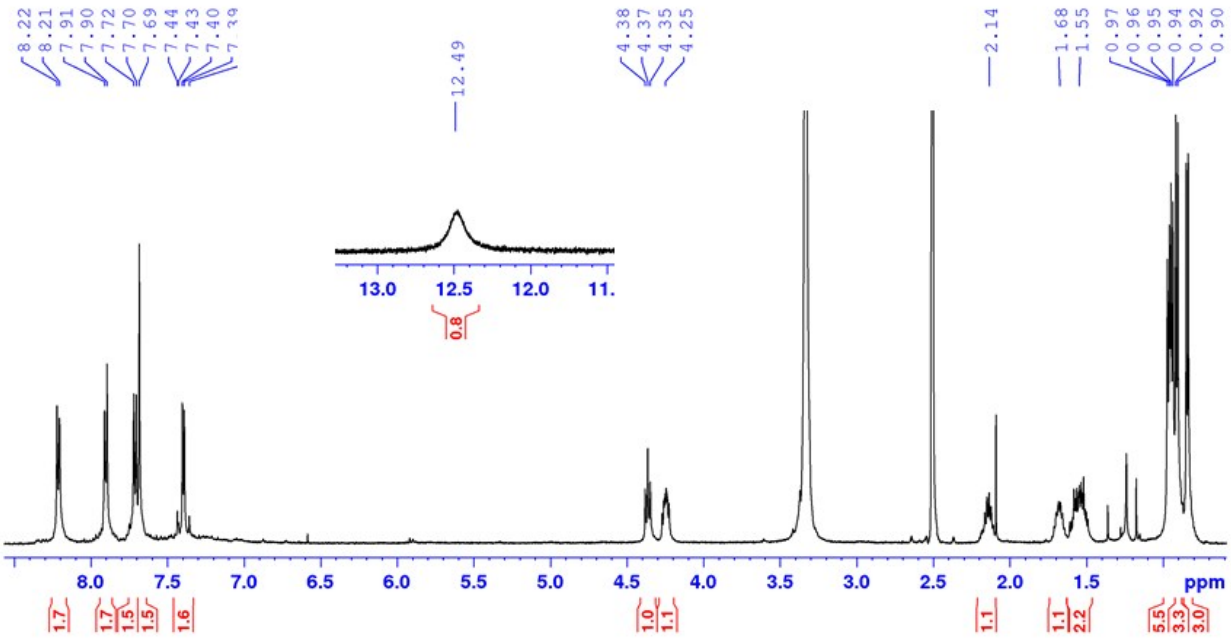

Figure S1. [1]H NMR (500 MHz) of LMWG **1** in DMSO at room temperature.

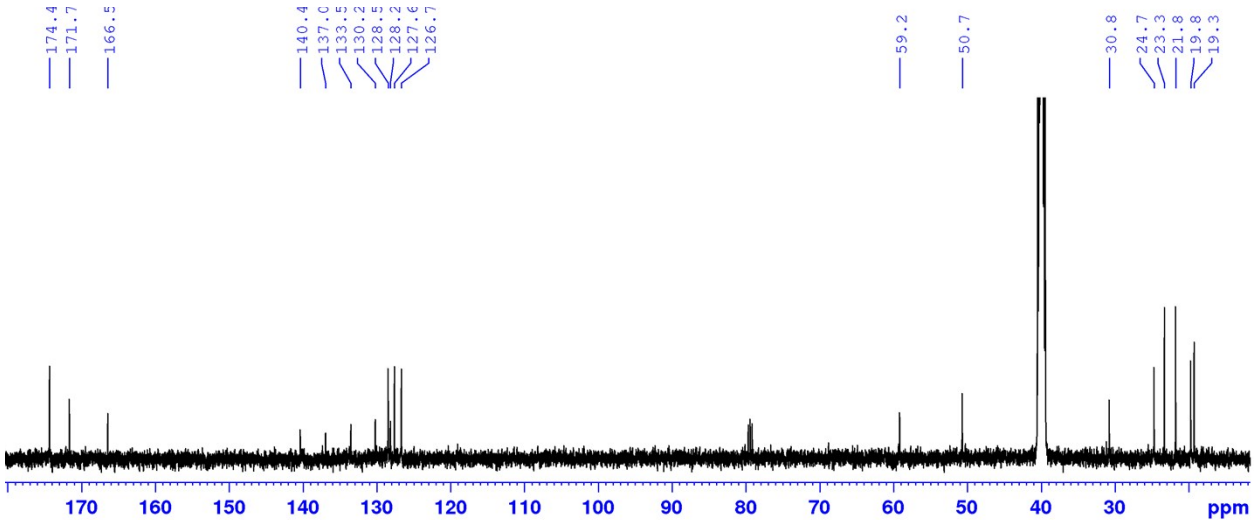

Figure S2. [13]C NMR (125 MHz) of LMWG **1** in DMSO at room temperature.

Synthesis of LMWG 2: OPV-3 diacid (577 mg, 1.5 mmol) was suspended in thionyl chloride (15 mL), added 2 drops of DMF and refluxed until the solid was completely dissolved (aprox. 16 h). The mixture was allowed to cool down to room temperature and evaporated under reduced pressure. A mixture of anhydrous DCM/NMP 2:1 (20 mL) and DMAP (catalytic amount) were added to the solid residue and stirred for 10 min. The mixture was cooled down to 0 ºC and a solution of L-valyl-L-phenylalanine methyl ester trifluoroacetate salt (1.34 gr, 3.4 mmol) and triethylamine (1.2 mL, 8.5 mmol) in dry DCM (5mL) was added dropwise. The resulting mixture was allowed to stir

overnight at room temperature under N_2. The day after the DCM was evaporated under reduced pressure and water added to the resulting dark liquid residue. The solid formed was collected by filtration, washed thoroughly with water and dried under vacuum. The dried solid was then triturated with acid water, collected again by filtration and washed with water, methanol, dichloromethane, and dried under vacuum for 24 h to obtain the methyl protected gelator **2** as a dark yellow solid in 46% yield. This solid (630 mg, 0.7 mmol) was suspended in THF/H_2O 3:1 (20mL) and LiOH (0.35 gr) added. The resulting mixture was stirred overnight at room temperature. The day after the mixture was acidified with HCl 2M until pH ~ 3. The solid obtained was collected by filtration, thoroughly washed with water and dried under vacuum. Gelator **2** was obtained as a pale yellow solid (600 mg, 98% second step, 47% overall yield). ^{1}H NMR (DMSO, 500 MHz): δ = 12.68 (br, 1H), 8.28 (d, *J* = 8.4 Hz, 1H), 8.18 (d, *J* = 9.3 Hz, 1H), 7.89 (d, *J* = 8.3 Hz, 2H), 7.71 (d, *J* = 8.8 Hz, 2H), 7.69 (s, 2H), 7.43 (d, *J* = 15.2 Hz, 1H), 7.38 (d, *J* = 16.3 Hz, 1H), 7.24 (m, 2H), 7.21 (m, 2H), 7.15 (t, *J* = 7.0 Hz, 1H), 4.47 (m, 1H), 4.34 (t, *J* = 5.5 Hz, 1H), 3.07 (dd, *J* = 5.3, 14.1 Hz, 1H), 2.93 (dd, *J* = 9.2, 14.1 Hz, 1H), 2.09 (sex, *J* = 7.0 Hz, 1H), 0.89 (t, *J* = 7.5 Hz, 6H); ^{13}C (DMSO, 125 MHz): δ = 173.2, 171.5, 166.3, 140.4, 137.9, 136.9, 133.5, 130.2, 129.6(2C), 128.6(2C), 128.5(2C), 128.2, 127.6(2C), 126.8, 126.6(2C), 59.3, 53.8, 37.2, 30.7, 19.7, 19.3. ESI-MS (negative): *m*/*z* 861 ([M−H]$^-$).

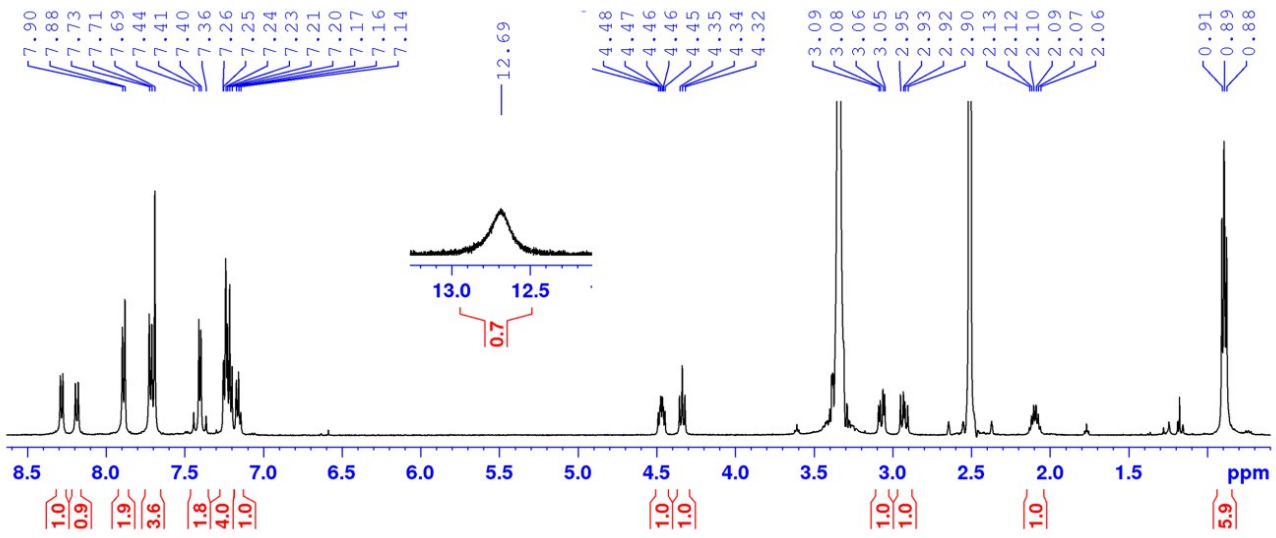

Figure S3. ^{1}H NMR (500 MHz) of LMWG **2** in DMSO at room temperature.

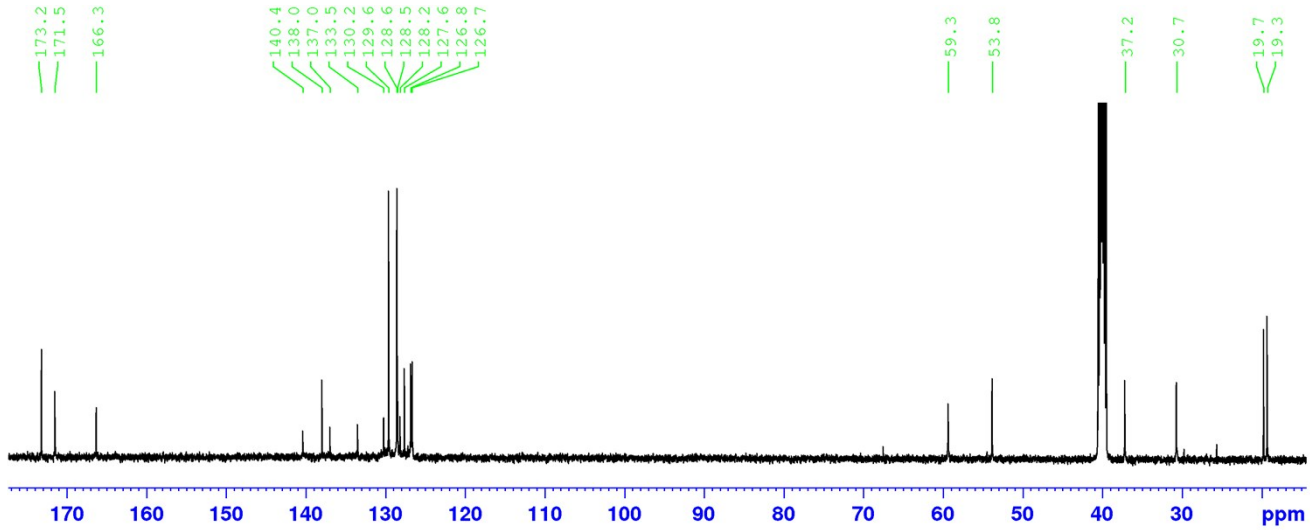

Figure S4. ^{13}C NMR (500 MHz) of LMWG **2** in DMSO at room temperature.

Synthesis of S1. OPV-3 diacid (212 mg, 0.57 mmol) was suspended in thionyl chloride (5 mL) and refluxed until the solid was completely dissolved (aprox. 8 h). The mixture was allowed to cool down to room temperature and evaporated under reduced pressure. A solution of glycine methyl ester hydrochloride (216 mg, 1.7 mmol), NMM (260 μL, 2.3 mmol) and DMPA (catalytic amount) in DCM (15 mL) was added dropwise to the solid residue while the flask is kept in an ice bath. The resulting mixture was allowed to stir overnight at room temperature under N_2. The day after the mixture was filtrated and the solid collected washed with basic water, DCM, methanol and dried under vacuum to obtain the methyl protected gelator in 49% yield. This solid (143 mg, 0.28 mmol) was suspended in THF/EtOH/H_2O 3:1:1 (10 mL) and LiOH (0.3 gr) added. The resulting mixture was stirred overnight at room temperature. The day after the mixture was acidified with HCl 2M until pH ~ 3. The solid obtained was collected by filtration, thoroughly washed with water and dried under vacuum. **S1** was obtained as a pale yellow solid (100 mg, 74% second step, 36% overall yield). ^{1}H NMR (DMSO, 500 MHz): δ = 12.61 (br, 1H), 8.83 (t, J = 5.9 Hz, 1H), 7.89 (d, J = 8.7 Hz, 2H), 7.72 (d, J = 8.7 Hz, 2H), 7.67 (s, 2H), 7.42 (d, J = 16.3 Hz, 1H), 7.37 (d, J = 16.8 Hz, 1H), 3.93 (d, J = 5.8 Hz, 2H); ^{13}C (DMSO, 125 MHz): δ = 171.8, 166.5, 140.5, 137.0, 133.0, 130.4, 128.2(2C), 128.1, 127.6(2C), 126.8(2C), 41.7. **S1** is only soluble in hot DMSO and therefore no ESI-MS data could be collected.

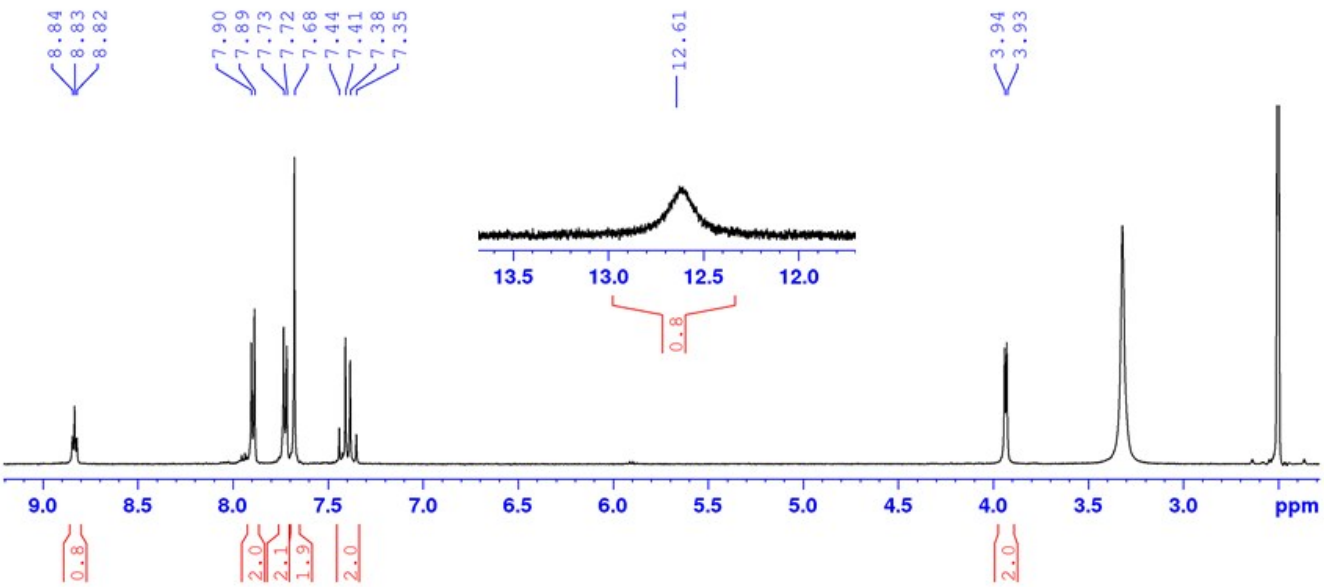

Figure S5. ^{1}H NMR (500 MHz) of **S1** in DMSO at room temperature.

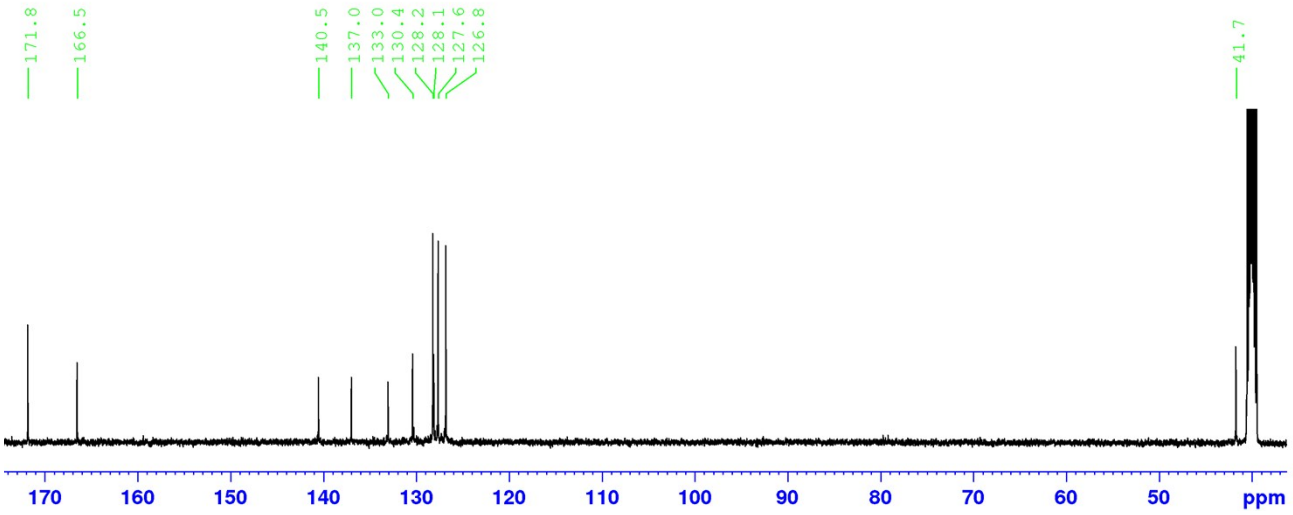

Figure S6. ^{13}C NMR (125 MHz) of **S1** in DMSO at room temperature.

Synthesis of S2. OPV-3 diacid (0.4 gr, 1.0 mmol) was suspended in thionyl chloride (8 mL), added 2 drops of DMF and refluxed until the solid was completely dissolved (aprox. 16 h). The mixture was allowed to cool down to room temperature and evaporated under reduced pressure and dichloromethane (5 mL) was added to the solid residue. The resulting mixture was cooled down to 0 ºC and a solution of L-valine ethyl ester hydrochloride (0.43 gr, 2.4 mmol) and NMM (0.3 mL, 2.7 mmol) in DCM was added dropwise. The resulting mixture was allowed to stir overnight at room temperature under N_2. The day after the mixture was evaporated under reduced pressure, the resulting

solid redissolved in hot DCM and filtrated while still hot. The filtrate was rotary-evaporated and the residue triturated with MeOH, collected by filtration and dried under vacuum to obtain methyl protected **S2** as a pale yellow solid (165 mg, 26%). This solid (165 mg, 0.27 mmol) was suspended in THF/H_2O 3:1 (16mL) and LiOH (0.3 gr) added. The resulting mixture was stirred overnight at room temperature. The day after the mixture was acidified with HCl 2M until pH ~ 3. The solid obtained was collected by filtration, thoroughly washed with water and dried under vacuum. **S2** was obtained as a pale yellow solid (140 mg, 89% yield for the second step, 23% overall yield). ^{1}H NMR (DMSO, 500 MHz): δ = 12.60 (br, 1H), 8.41 (d, *J* = 8.1 Hz, 1H), 7.92 (d, *J* = 8.4 Hz, 2H), 7.71 (d, *J* = 8.4 Hz, 2H), 7.68 (s, 2H), 7.42 (d, *J* = 16.3 Hz, 1H), 7.37 (d, *J* = 16.4 Hz, 1H), 4.29 (t, *J* = 7.5 Hz, 1H), 2.20 (sext, *J* = 6.7 Hz, 1H), 0.99 (d, *J* = 6.5 Hz, 3H), 0.97 (d, *J* = 6.7 Hz, 3H); ^{13}C (DMSO, 125 MHz): δ = 173.6, 166.9, 140.4, 137.0, 133.3, 130.2, 128.6(2C), 128.2, 127.6(2C), 126.6(2C), 58.8, 29.9, 19.8, 17.3. ESI-MS (positive): *m*/*z* 635 ([M−2H+3Na]$^+$).

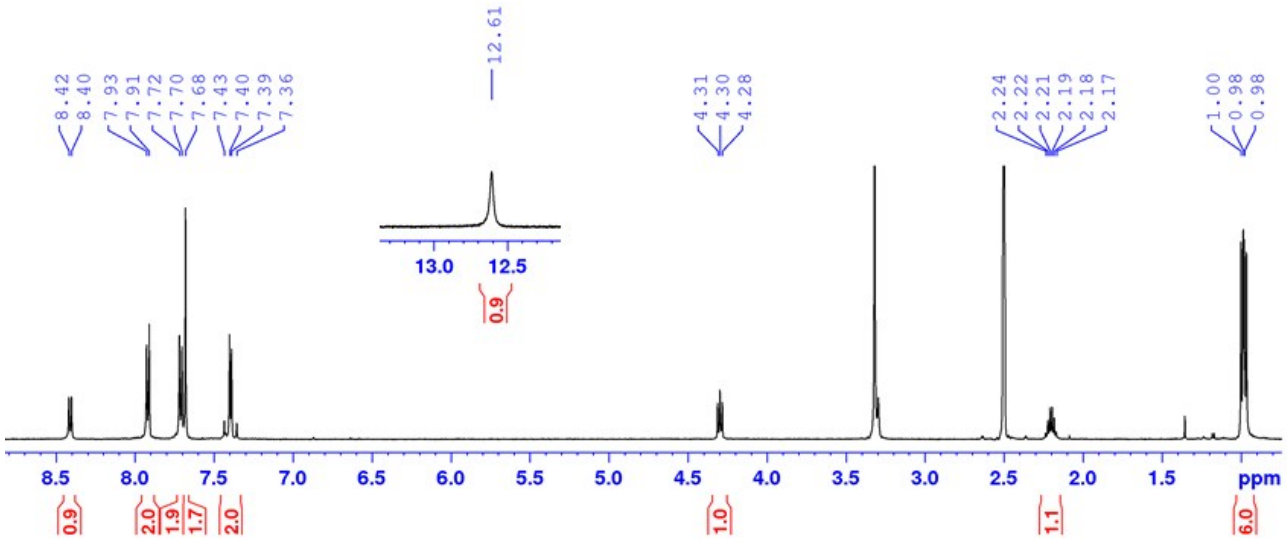

Figure S7. ^{1}H NMR (500 MHz) of **S2** in DMSO at room temperature.

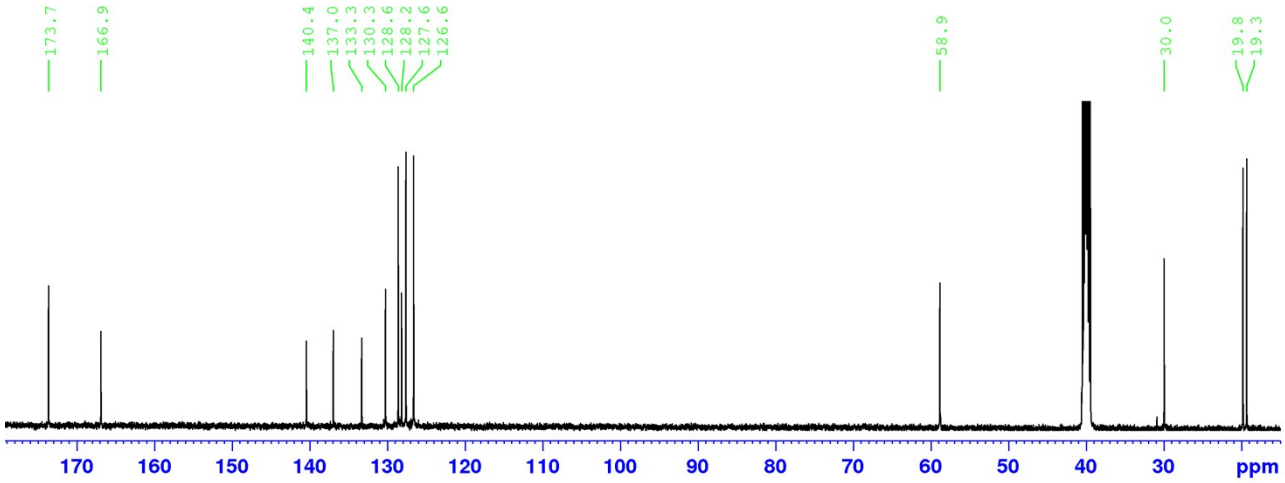

Figure S8. ^{13}C NMR (125 MHz) of **S2** in DMSO at room temperature.

Synthesis of S3. OPV-3 diacid (0.34 gr, 0.9 mmol) was suspended in thionyl chloride (5 mL) and refluxed until the solid was completely dissolved (aprox. 8 h). The mixture was allowed to cool down to room temperature and evaporated under reduced pressure. A solution of L-alanine methyl ester hydrochloride (0.27 gr, 1.9 mmol), NMM (0.5 mL, 4.5 mmol) and DMAP (catalytic amount) in DCM (15 mL) was added dropwise to the solid residue while the flask is kept in an ice bath. The resulting mixture was allowed to stir overnight at room temperature under N_2. The day after the mixture was filtrated and the solid collected washed with DCM and methanol, and dried under vacuum to obtain the dimethyl protected **S3** in 69% yield. This solid (300 mg, 0.55 mmol) was suspended in THF/H_2O 3:1 (8 mL) and LiOH (0.3 gr) added. The resulting mixture was stirred overnight at room temperature. The day after the mixture was acidified with HCl 2M until pH ~ 3. The solid obtained was collected by filtration, thoroughly washed with water and dried under vacuum. **S3** was obtained as a pale yellow solid (211 mg, 74% yield for the second step, 51% overall yield). ^{1}H NMR (DMSO, 500 MHz): δ = 12.55 (br, 1H), 8.66 (d, J = 7.1 Hz, 1H), 7.92 (d, J = 8.5 Hz, 2H), 7.72 (d, J = 9.0 Hz, 2H), 7.68 (s, 2H), 7.43 (d, J = 16.0 Hz, 1H), 7.37 (d, J = 16.0 Hz, 1H), 4.43 (qn, J = 7.2 Hz, 1H), 1.41 (d, J = 7.3 Hz, 3H); ^{13}C (DMSO, 125 MHz): δ = 174.7, 166.2, 140.5, 137.0, 133.1, 130.3, 128.4(2C), 128.1, 127.6(2C), 126.7(2C), 48.6, 17.4. ESI-MS (positive): m/z 579 ([M−2H+3Na]$^+$).

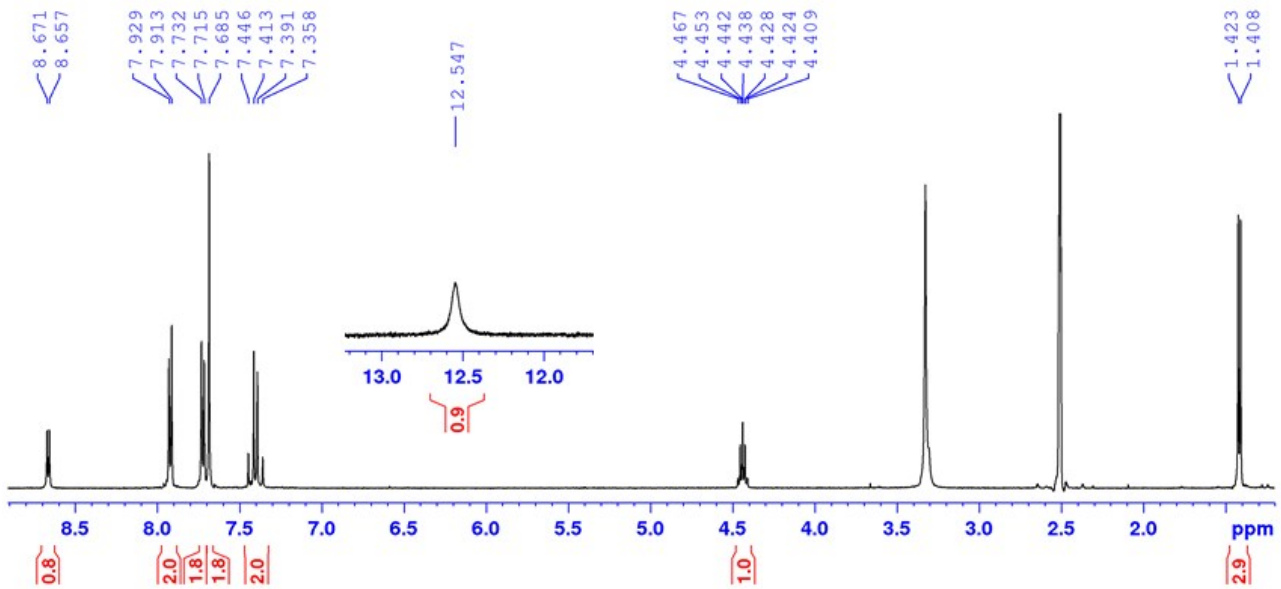

Figure S9. ^{1}H NMR (500 MHz) of **S3** in DMSO at room temperature.

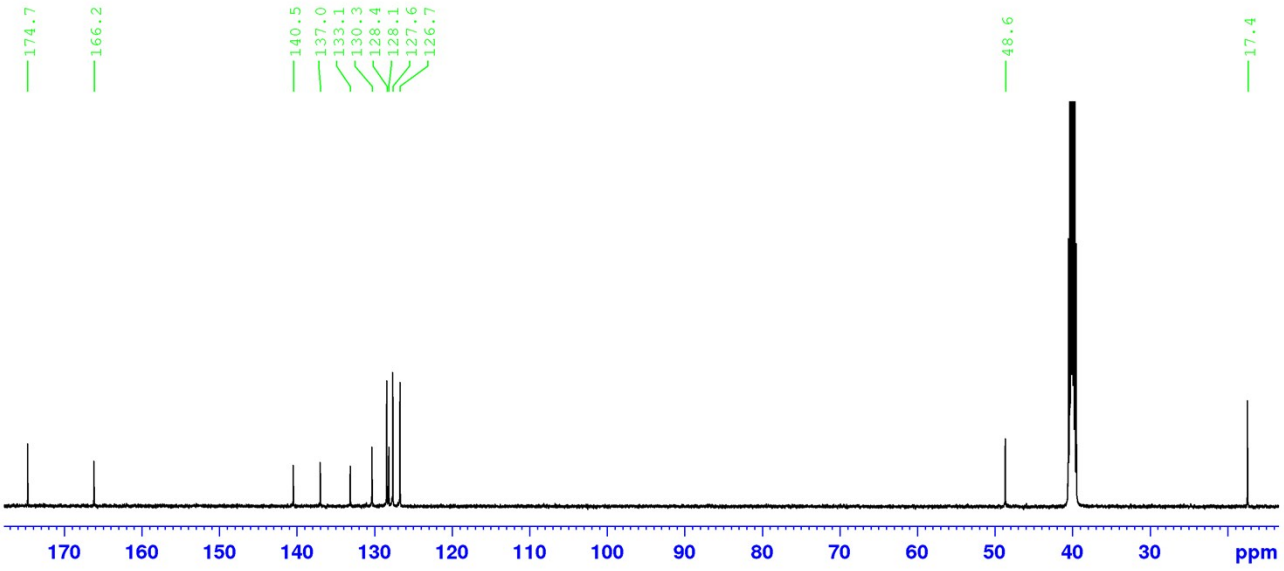

Figure S10. ^{13}C NMR (125 MHz) of **S3** in DMSO at room temperature.

Synthesis of S4. OPV-3 diacid (0.41 gr, 1.1 mmol) was suspended in thionyl chloride (6 mL) and refluxed until the solid was completely dissolved (aprox. 8 h). The mixture was allowed to cool down to room temperature and evaporated under reduced pressure. A solution of L-phenylalanine methyl ester hydrochloride (0.5 gr, 2.3 mmol) and NMM (0.6 mL, 5.4 mmol) in DCM (15 mL) was added dropwise to the solid residue while the flask was kept in an ice bath. The resulting mixture was allowed to stir overnight at room temperature under N_2. The day after the mixture was evaporated under reduced pressure, the resulting solid redissolved in hot DCM and filtrated while still hot. The solid collected was extensively washed with hot DCM. The filtrate was rotary-evaporated, redissolved

in the minimum amount of hot DCM and MeOH added. The day after the solid precipitated was collected and dried under vacuum to obtain the dimethyl protected **S4** in 35% yield. This solid (268 mg, 0.38 mmol) was suspended in THF/H_2O 3:1 (16 mL) and LiOH (0.3 gr) added. The resulting mixture was stirred overnight at room temperature. The day after the mixture was acidified with HCl 2M until pH ~ 3. The solid obtained was collected by filtration, thoroughly washed with water and dried under vacuum. **S4** was obtained as a pale yellow solid (231 mg, 90% yield for the second step, 31% overall yield). ^{1}H NMR (DMSO, 500 MHz): δ = 12.77 (br, 1H), 8.70 (d, *J* = 8.2 Hz, 1H), 7.83 (d, *J* = 8.3 Hz, 2H), 7.70 (d, *J* = 8.4 Hz, 2H), 7.67 (s, 2H), 7.41 (d, *J* = 16.7 Hz, 1H), 7.37 (d *overlapping with Phe signals*, 1H), 7.33 (d, *J* = 7.3 Hz, 2H), 7.28 (t, *J* = 7.6 Hz, 2H), 7.19 (t, *J* = 7.2 Hz, 1H), 4.63 (m, 1H), 3.21 (dd, *J* = 4.5, 13.9 Hz, 1H), 3.09 (dd, *J* = 10.7, 14.0 Hz, 1H); ^{13}C (DMSO, 125 MHz): δ = 173.7, 166.4, 140.5, 138.7, 136.9, 133.1, 130.3, 129.5 (2C), 128.7(2C), 128.3(2C), 128.1, 127.6(2C), 126.8, 126.7(2C), 54.7, 36.7. ESI-MS (positive): *m*/*z* 731 ([M−2H+3Na]$^+$).

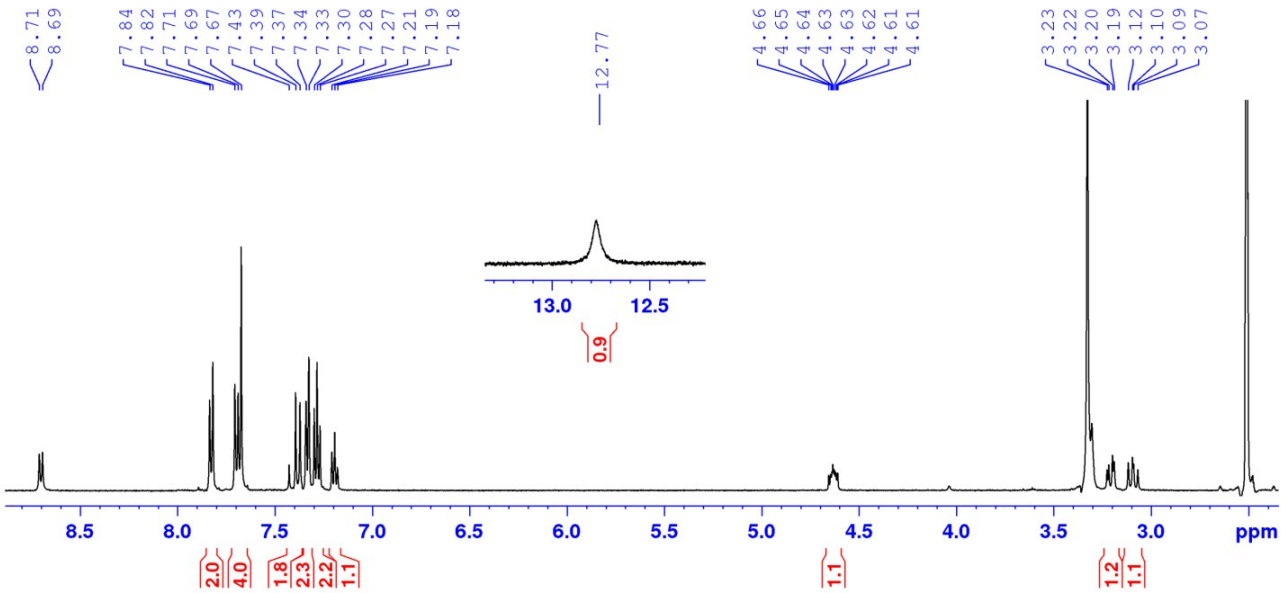

Figure S11. ^{1}H NMR (500 MHz) of **S4** in DMSO at room temperature.

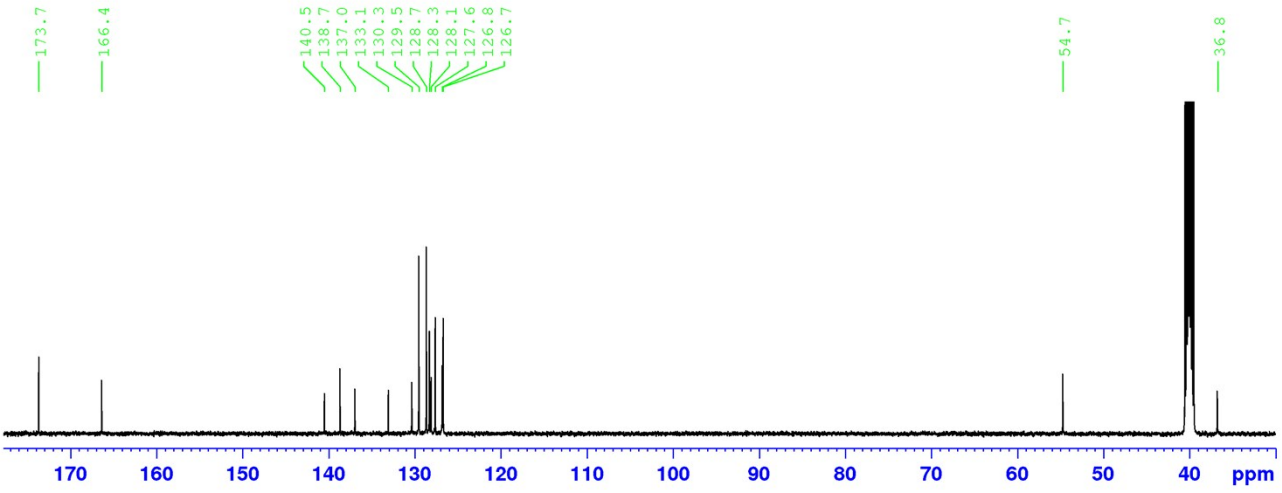

Figure S12. ^{13}C NMR (125 MHz) of **S4** in DMSO at room temperature.

2. Supporting figures

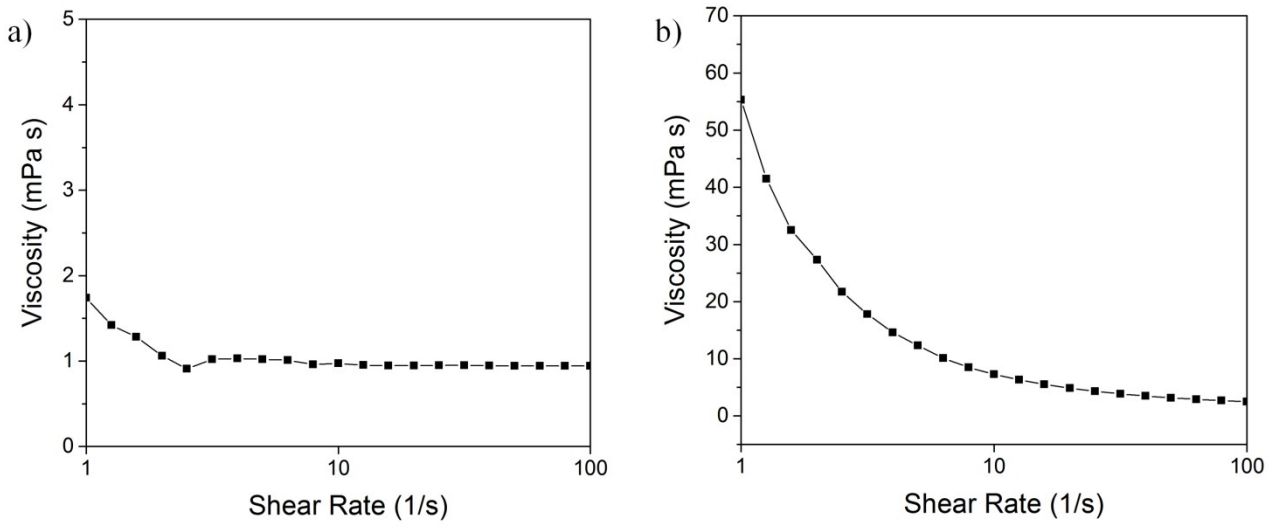

Figure S13. Viscosity measurements for solutions of a) gelator **1** and b) gelator **2** under increasing shear rate. Concentration = 5 mg/mL, pH = 10.2.

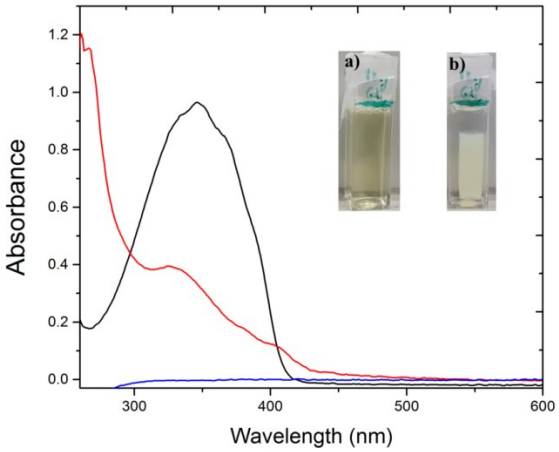

Figure S14. UV-Vis spectra of a) a solution of **1** (5mg/mL) at pH = 10 after dilution to 0.03 mM (black trace), and the liquid exuded upon syneresis of the gel formed after 72 h of addition of GdL (6mg/mL) to the initial solution of **1** b) without diluting (red trace) and c) after diluting to 0.03 mM (blue trace). The inset photographs show (a) the initial solution of **1** at high pH and (b) the syneresed gel formed after 72 h of the addition of GdL, the liquid expelled was measured to be 60% of the volume of the initial solution.

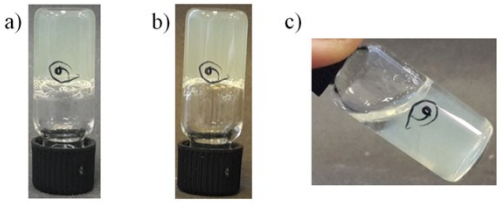

Figure S15. Photographs showing the gels formed 24 hours (a), 4 days (b) and 5 days (c) after the addition of GdL (6mg/mL) to an aqueous solution of gelator **2** (5mg/mL, pH = 10).

Figure S16. Photographs showing the progress of gelation and syneresis after addition of GdL (3mg/mL) to a solution of **1** (5mg/mL, pH = 10) containing bromophenol blue (t = 0).

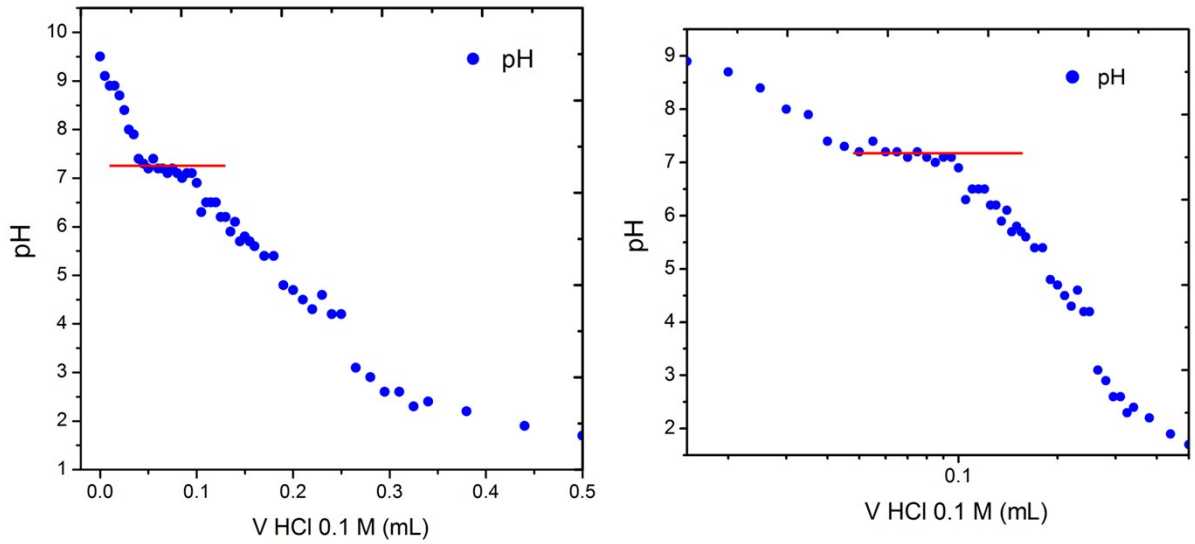

Figure S17. Titration curve of an aqueous solution of **2** (5mg/mL, initial pH = 10) with HCl 0.1 M plotted in linear scale (left) and in logarithmic scale (right). Red lines in the graphs denote the apparent pK_a found for **2**.

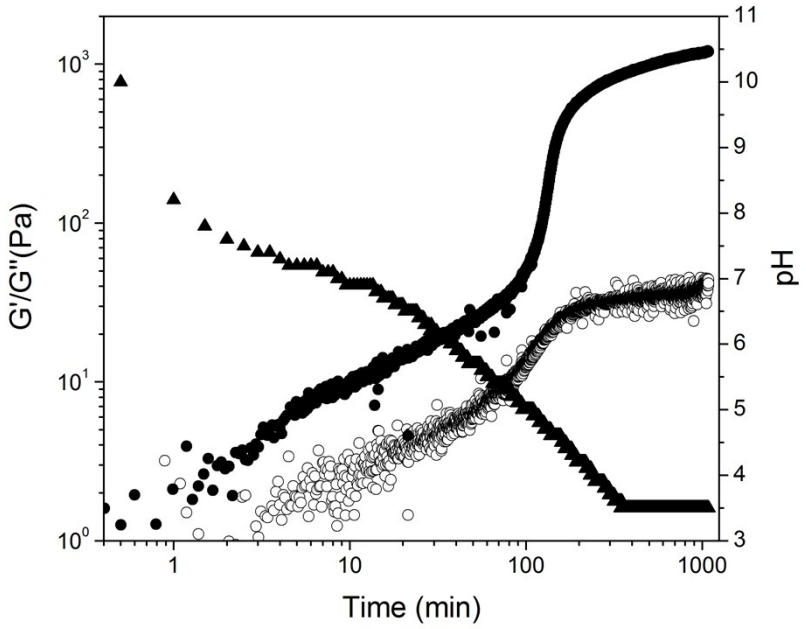

Figure S18. Evolution of pH (triangles), G′ (full circles) and G″ (open circles) with time after the addition of 5mg/mL of GdL to a solution of gelator **2** (5 mg/mL, pH = 11). Rheology measurements were carried out at a strain of 0.5 % and a frequency of 10 rad/s at 25 °C.

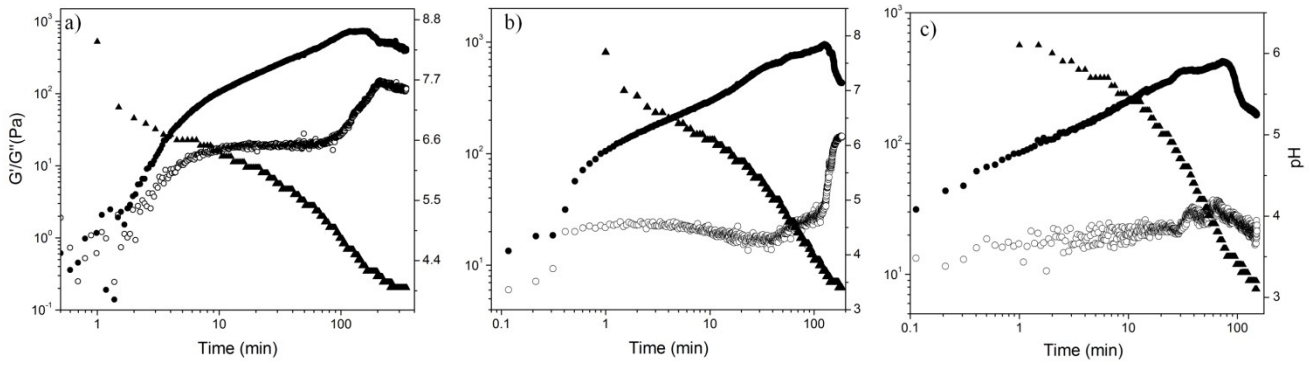

Figure S19. Evolution of pH (triangles), G′ (full circles) and G″ (open circles) with time after the addition of 6mg/mL of GdL to a 3 mg/mL solution of gelator **1** at a) pH = 12, b) pH = 10 and c) pH = 7. These data were used to construct Figure 4 of the manuscript. Rheology measurements were carried out at a strain of 0.5 % and a frequency of 10 rad/s at 25 °C.

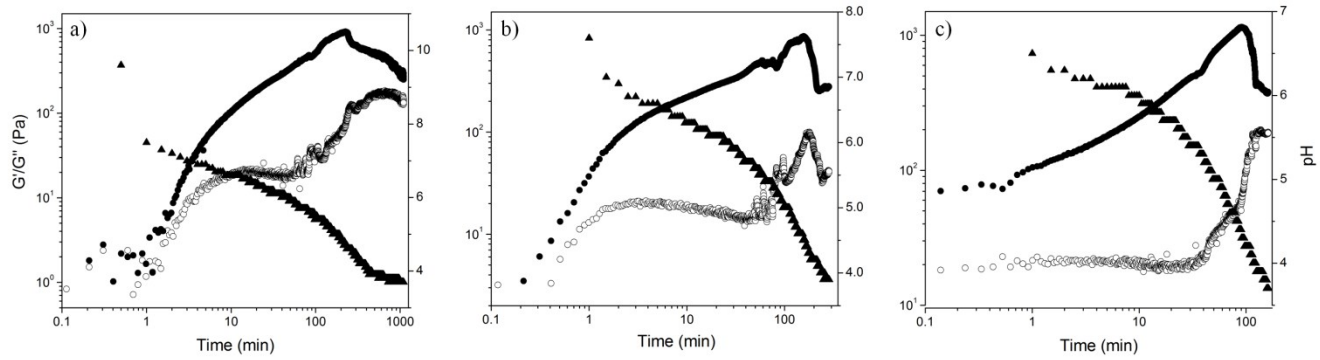

Figure S20. Evolution of pH (triangles), G′ (full circles) and G″ (open circles) (open circles) with time after the addition of 6mg/mL of GdL to a 5 mg/mL solution of gelator **1** at a) pH = 12, b) pH = 10 and c) pH = 7. These data were used to construct Figure 4 of the manuscript. Rheology measurements were carried out at a strain of 0.5 % and a frequency of 10 rad/s at 25 °C.

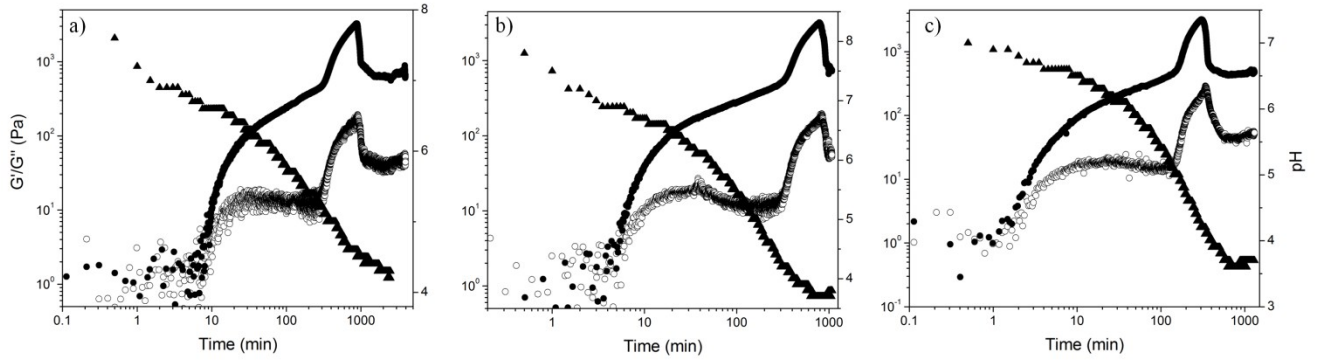

Figure S21. Evolution of pH (triangles), G′ (full circles) and G″ (open circles) with time after the addition of 6mg/mL of GdL to a 10 mg/mL solution of gelator **1** at a) pH = 12, b) pH = 10 and c) pH = 7. These data were used to construct Figure 4 of the manuscript. Rheology measurements were carried out at a strain of 0.5 % and a frequency of 10 rad/s at 25 °C.

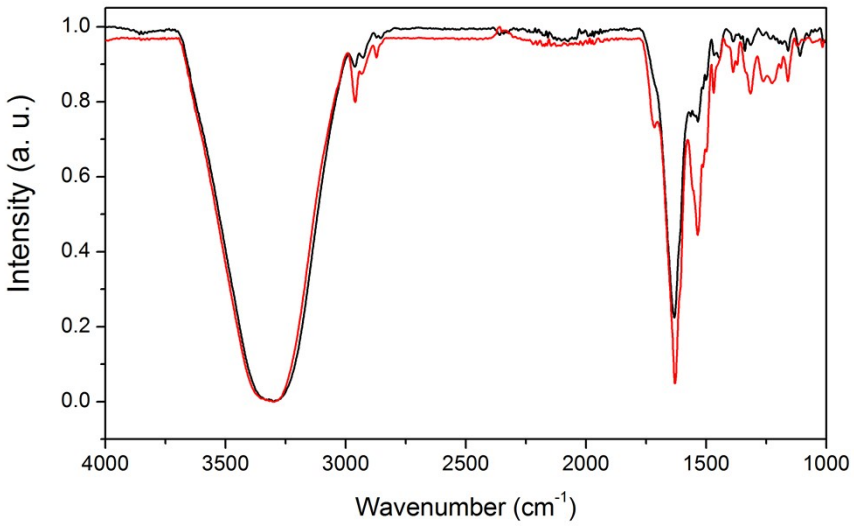

Figure S22. Infrared spectrum of the syneresed (red) and non-syneresed gels (black) of **1**. The data has been normalised to unity.

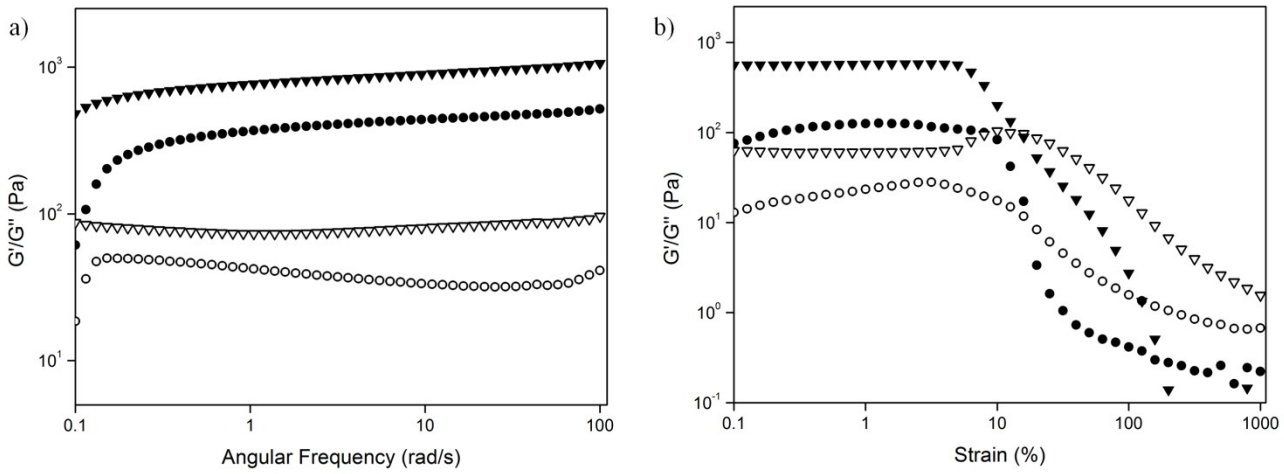

Figure S23. a) Frequency and b) strain sweeps for gelator **1** before (circles) and after (triangles) shrinking. In all cases, full symbols represent G' and open circles represent G''. Several gel samples were prepared in plastic moulds from 1.5 mL of a solution of gelator **1** (5 mg/mL, pH = 10) and 3 mg/mL of GdL. Frequency and strain sweeps of the first samples were measured 6 hours after adding GdL, when a self-supporting gel was observed to have formed but not yet syneresed (circles). After 24 hours, frequency and strain sweeps of the rest of the gel samples were measured, when the gel had already undergone syneresis. For syneresed samples the exuded fluid was removed before transferring the gel onto the rheometer plate.

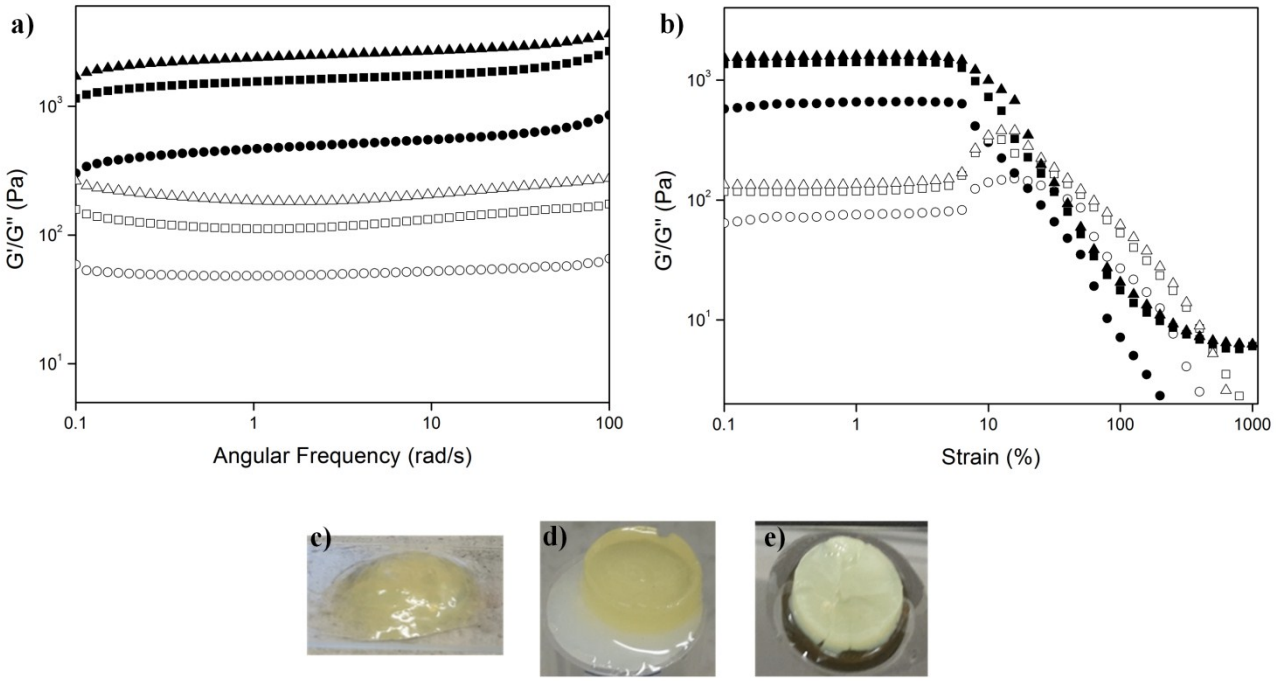

Figure S24. Top: comparison of a) frequency and b) strain sweeps for synerised hydrogels of **1** prepared using different amounts of GdL. Gel samples were prepared in plastic moulds from 2 mL of a solution of gelator **1** (5 mg/mL, pH 10) and 3 mg/mL (circles), 6 mg/mL (squares) or 10 mg/mL (triangles) of GdL. In all cases, full symbols represent G′ and open circles represent G″. In all cases, frequency and strain sweeps were measured 48 h after the addition of GdL. Bottom: photographs of the gels, prepared with c) 3, d) 6 and e) 10 mg/mL of GdL, used for measurements above. For syneresed samples the exuded fluid was removed before transferring the gel onto the rheometer plate.

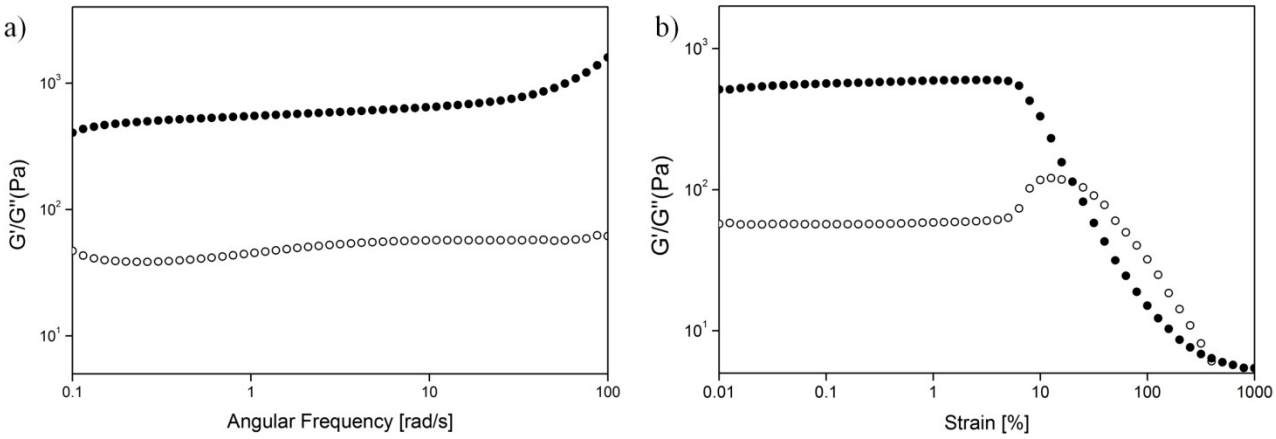

Figure S25. a) Frequency and b) strain sweeps for hydrogel **2**. Full circles represent G′ and open circles represent G″. Several gel samples were prepared in plastic moulds from a 5 mg/mL gelator **2** solution (1.5 mL) at pH 10 and 5 mg/mL of GdL.

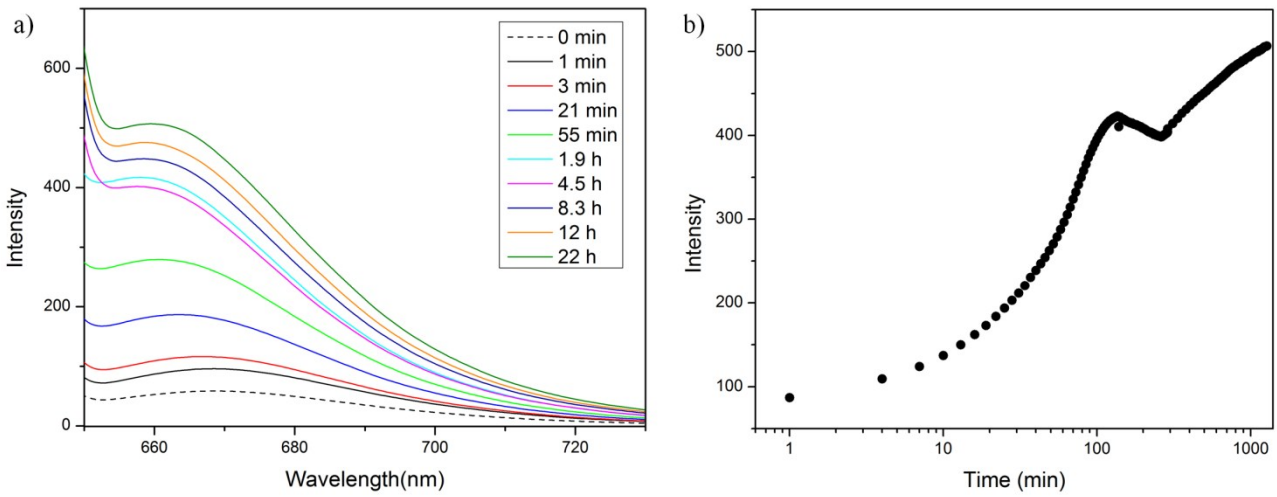

Figure S26. a) Changes in fluorescence of Nile blue (λ_{ex} = 630 nm) in a solution of gelator **1** (5mg/mL, pH = 10) after the addition of GdL (6 mg/mL). b) Plot of changes in fluorescence at 660 nm with time in a logarithmic scale. These graphs show Nile blue interacts with the gel fibres.[S4]

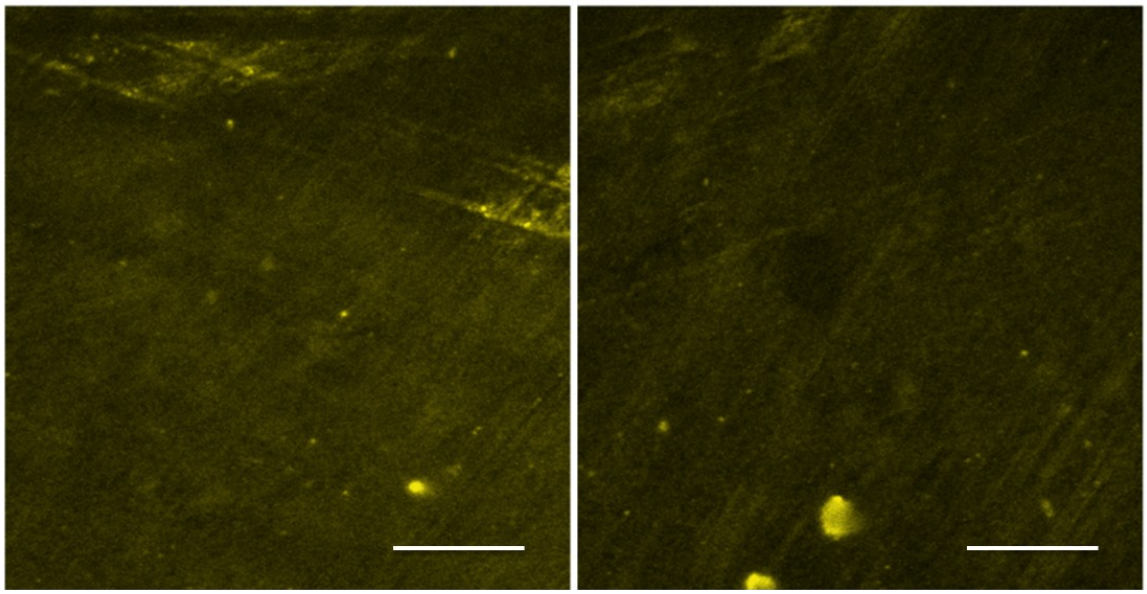

Figure S27. Representative confocal fluorescence microscopy images of non-syneresed gel of **1**. Scale bar is 20 μm. The large spherical objects are aggregates of Nile blue.

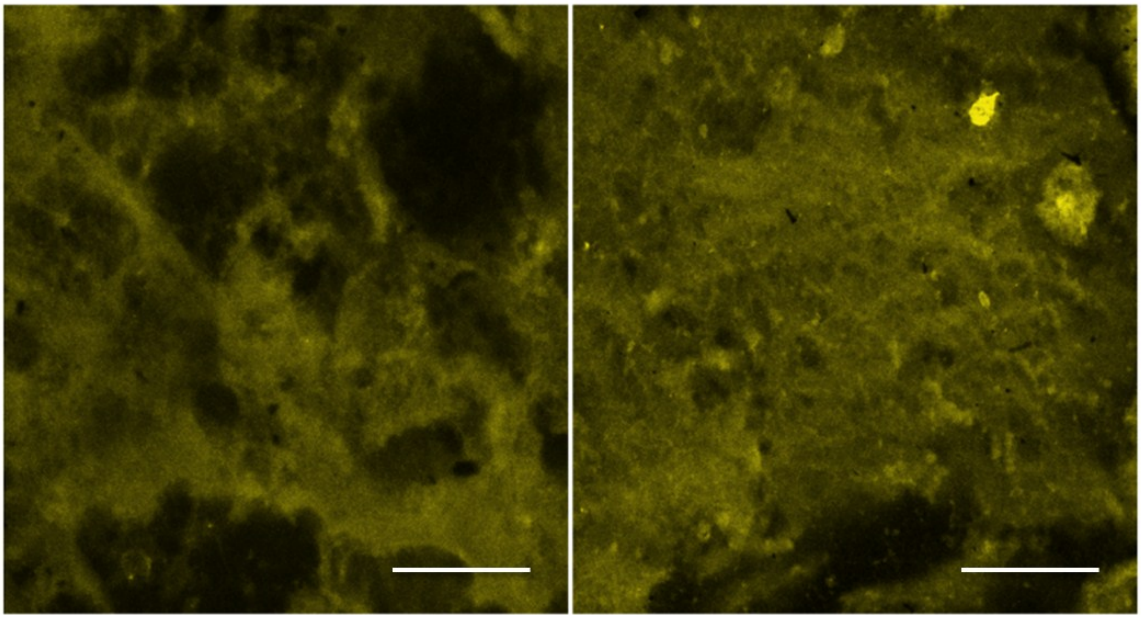

Figure S28. Representative confocal fluorescence microscopy images of syneresed gel of **1**. Scale bar is 20 μm. The large spherical objects are aggregates of Nile blue.

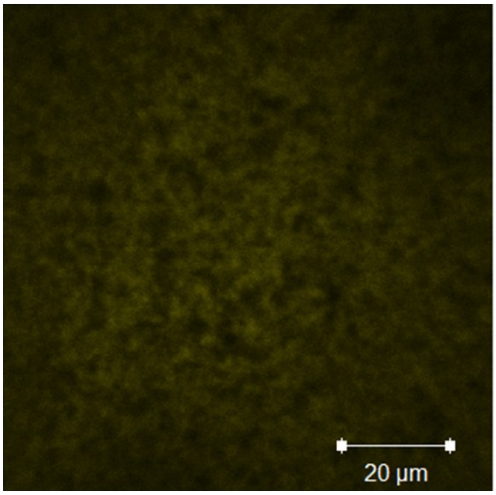

Figure S29. Representative confocal fluorescence microscopy images of the gel of **2**. Scale bar is 20 μm.

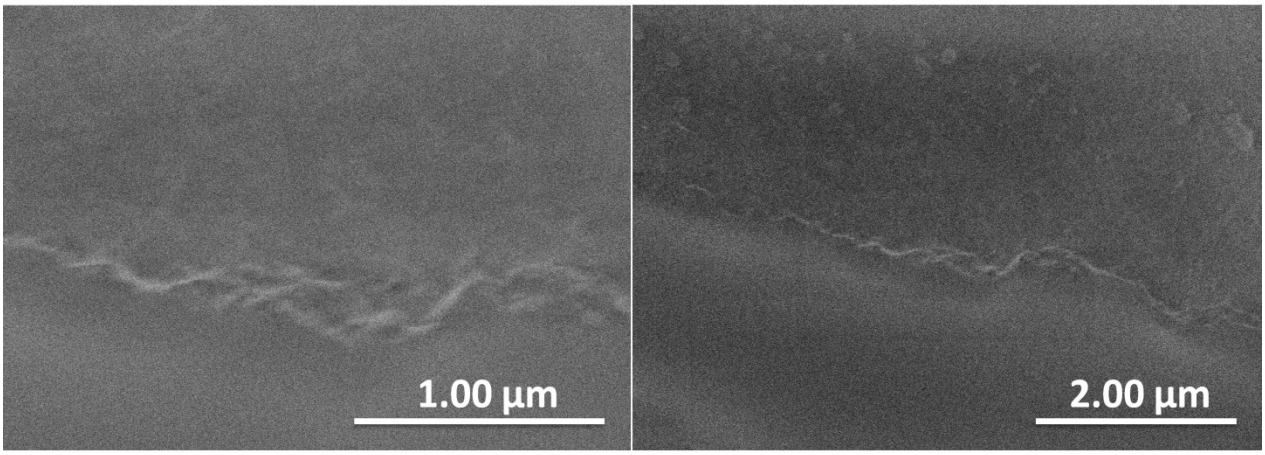

Figure S30. Representative SEM images of the non-syneresed gel of **1**.

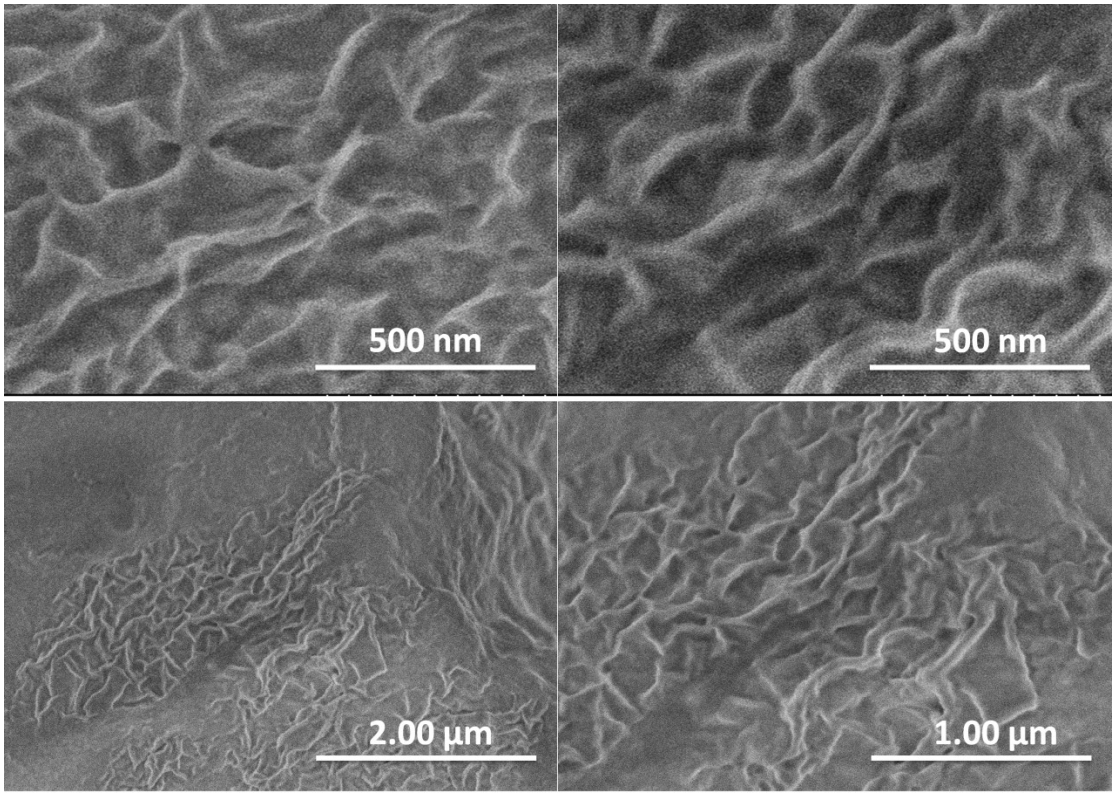

Figure S31. Representative SEM images of the syneresed gel of **1**.

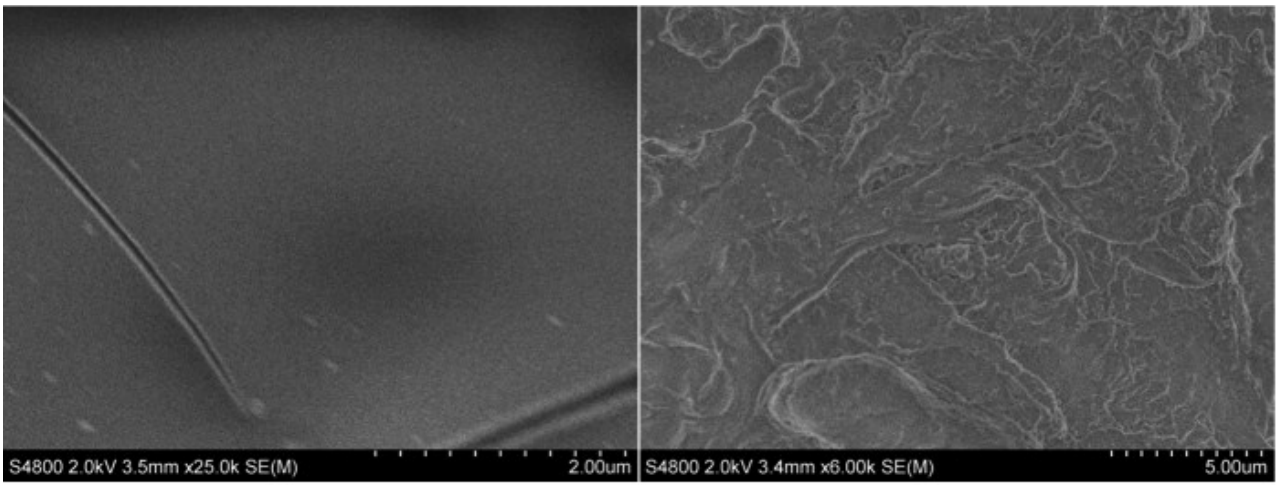

Figure S32. Example SEM image of (left) the solution of **2** at high pH and (right) the gel of **2** at low pH.

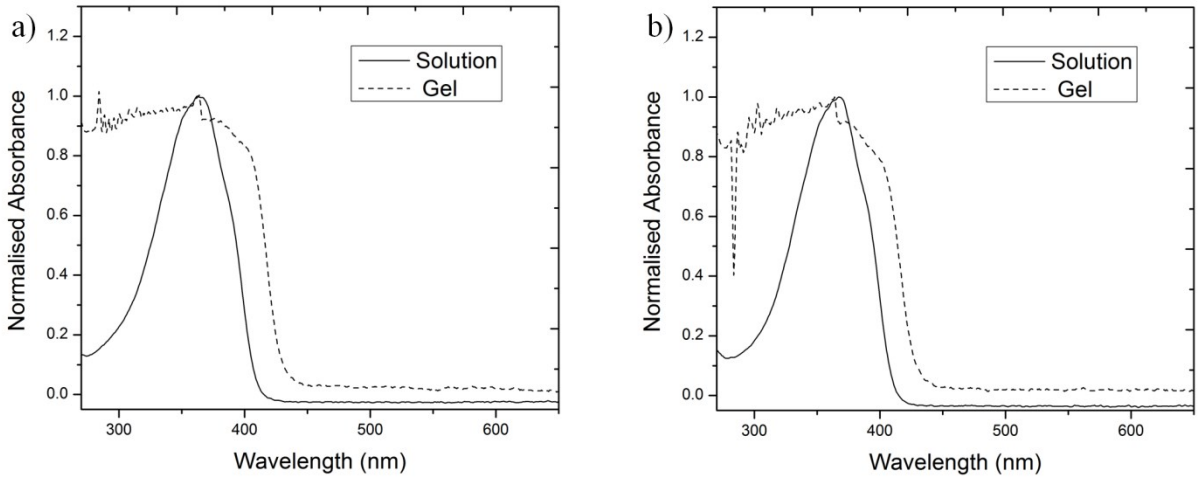

Figure S33. UV-Vis spectra of the solution and the hydrogel of a) gelator **1** and b) gelator **2**. Solutions of the gelators (5mg/mL) were prepared and then diluted to 0.02 mM with water (1 cm path length cuvette was used for measurements). Gels were prepared and transferred to a cuvette (0.1 mm path length demountable quartz cuvette) while still liquid. The cuvette was sealed with Parafilm and the sample allowed to gel before recording the UV-Vis spectra.

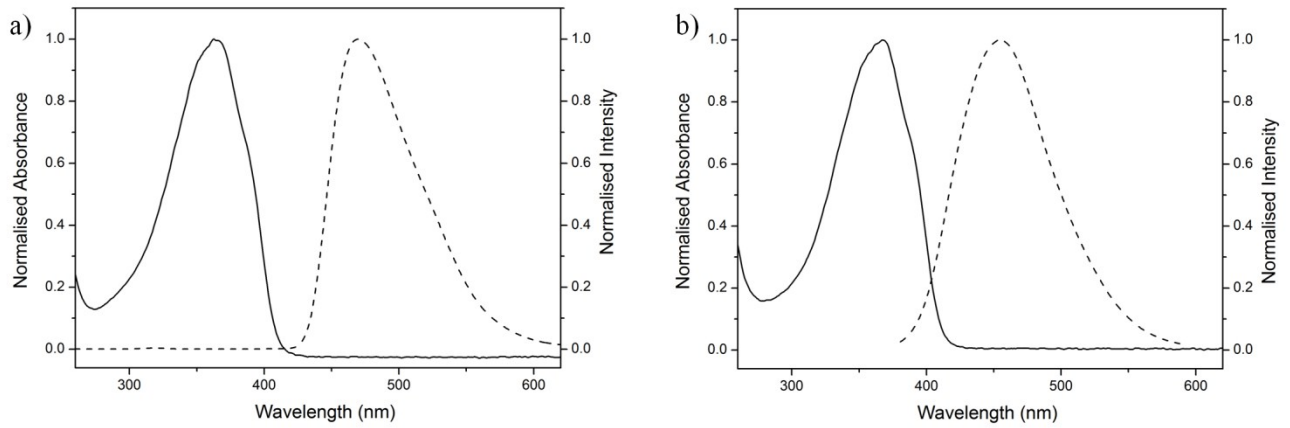

Figure S34. Absorption (black trace) and emission (black dashed trace) spectra of solutions of a) gelator **1** and b) gelator **2**. The solutions (5mg/mL) were prepared as described and then diluted. λ_{ex} = 320-350 nm.

3. NMR time-series measurements

The NMR data of Figure 6 was collected on a Bruker AvanceII 400 MHz wide bore spectrometer. All measurements were performed off lock in H_2O at 298 K. ^2H spectra were recorded *via* the lock channel with 3930 data points, an 8 ppm sweep width, a 200 μs pulse (70°) and 512 scans giving a total acquisition time of 35 minutes. No apodisation was applied to the raw FIDs prior to Fourier transformation. Lorentzian curves were fitted to the experimental peaks using the deconvolution function of Bruker Topspin 3.2. ^{23}Na T_1 and T_2 relaxation times were measured using the inversion-recovery and CPMG pulse sequences respectively. For T_1, the inversion recovery time, t, was varied between 1 and 300 ms in 8 steps. For T_2, the spacing between the π pulses was fixed at 1 ms and the number of pulses varied between 2 and 256 in 8 steps. 32 scans were collected in 6144 points with a 100 ppm sweep width and a relaxation delay of 0.1 s, giving an acquisition time of 2 minutes for both T_1 and T_2 measurements. For each sample, the ^{23}Na π/2 pulse was calibrated at high pH prior to the addition of GdL using the Bruker optimisation procedure POPT, typical π/2 pulses being 33 μs in duration. ^{23}Na T_1 and T_2 relaxation times were obtained by fitting the experimental curves to equations S1 and S2 respectively:

$$I = I_0\left[1 - P.exp\left(-{}^{t}/_{T_1}\right)\right] \quad \text{(S1)}$$

$$I = I_0 exp\left(-{}^{t}/_{T_2}\right) \quad \text{(S2)}$$

where I is the measured signal intensity, t is the time since initial excitation of the magnetization, P ≈ 1.9 and I_0 is a fitting parameter representing the signal intensity at t = 0. Example fits are shown on Figure S36.

The hydrogels were prepared as described in H_2O at 5 mg/mL gelator and 4 mg/mL GdL, the starting pH of the solution being 10.0. Dioxane-d_8 (0.05 vol%) was included as a probe for ^2H NMR. Sodium formate (1 mM), sodium acetate (0.5 mM), disodium methylphosphonate (0.5 mM) and sodium glycinate (0.5 mM) were also included as NMR pH indicators, with sodium methanesulfonate (0.2 mM) added as an internal reference. The pH time series on Figure 6 was calculated from the chemical shifts of these indicator molecules as described in our previous work.[S5]

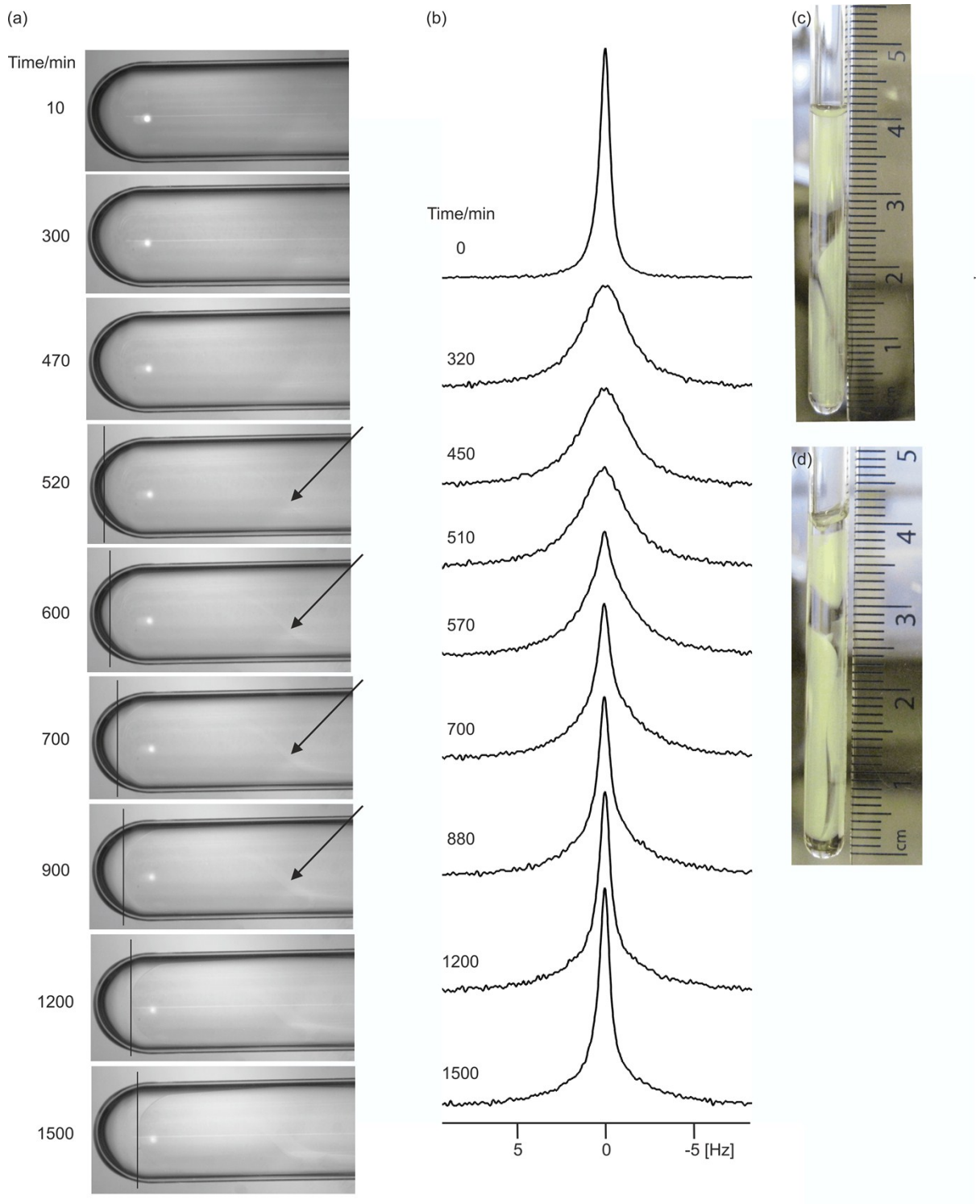

Figure S35. Parallel time-lapse photography and NMR spectroscopic analysis of formation and syneresis of a hydrogel of **1**. (a) Photographs of NMR tube in water bath at 298 K at times indicated since the addition of 4 mg/mL GdL to a solution of **1** at pH 10. The arrows indicate the location of a crack developing in the gel while the vertical lines indicate the position of the bottom of the gel. (b) ^{2}H NMR spectra of dioxane-d_8 in a parallel sample in the NMR spectrometer, fitted linewidths are shown on Figure 6a. Photographs of the samples 1600 minutes after the addition of GdL prepared in the NMR spectrometer (c) and in the water bath (d).

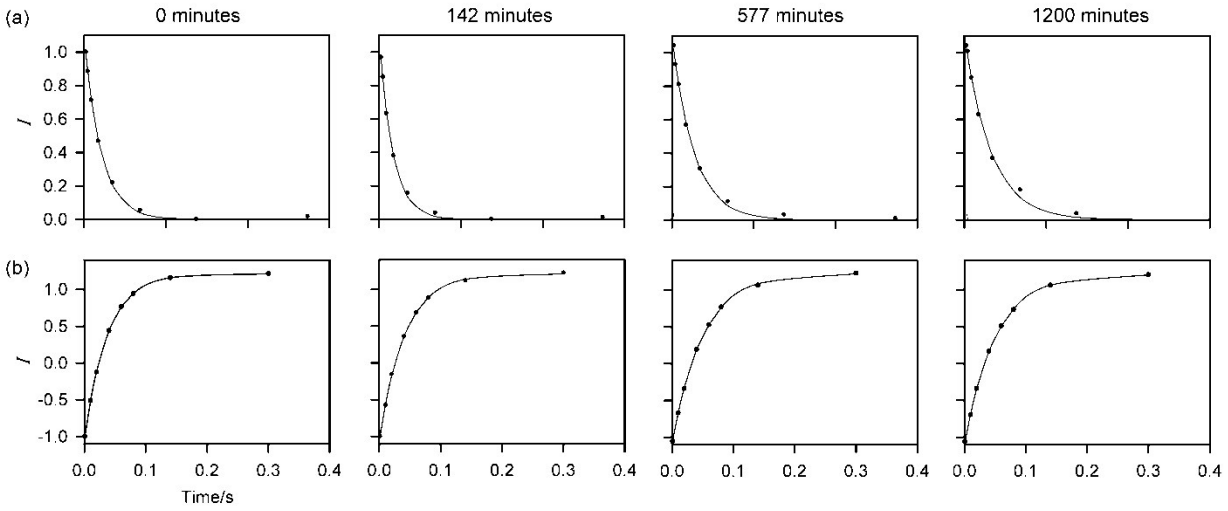

Figure S36. Example T_2 (a) and T_1 (b) $^{23}Na^+$ relaxation curves at times indicated since the addition of 4 mg/mL GdL to a solution of **1** at pH 10. Fits to equations S1 (T_1) and S2 (T_2) are shown as solid lines. Extracted T_1 and T_2 relaxation times are shown on Figure 6a. The ^{23}Na relaxation is essentially monoexponential at all times.

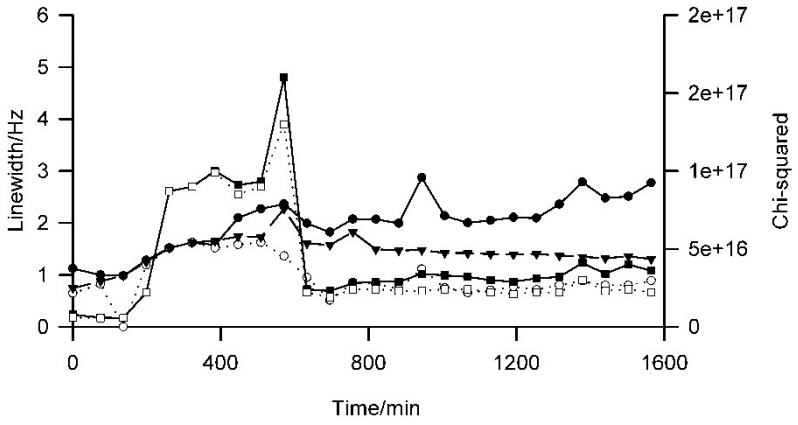

Figure S37. Plot of fitted ^2H linewidths of HDO as a function of time since addition of 4 mg/mL GdL to a solution of **1** at pH 10: single Lorentzian fit (black triangle), wider component of double Lorentzian fit (black circle) and narrow component (white circle). Quality of fits are indicated by their chi-squared values (smaller value represents better fit): single component fit (black square) and double component (white square). Unlike dioxane-d_8 (Figure 6b), the fitted linewidths increase only slightly with time. Following syneresis, a double Lorentzian fit is only marginally better than a single Lorentzian fit. The HDO signal arises from the natural abundance ^2H present in the water. The linewidth of HDO in an 0.05 vol% solution of dioxane-d_8 was measured as 0.7 Hz.

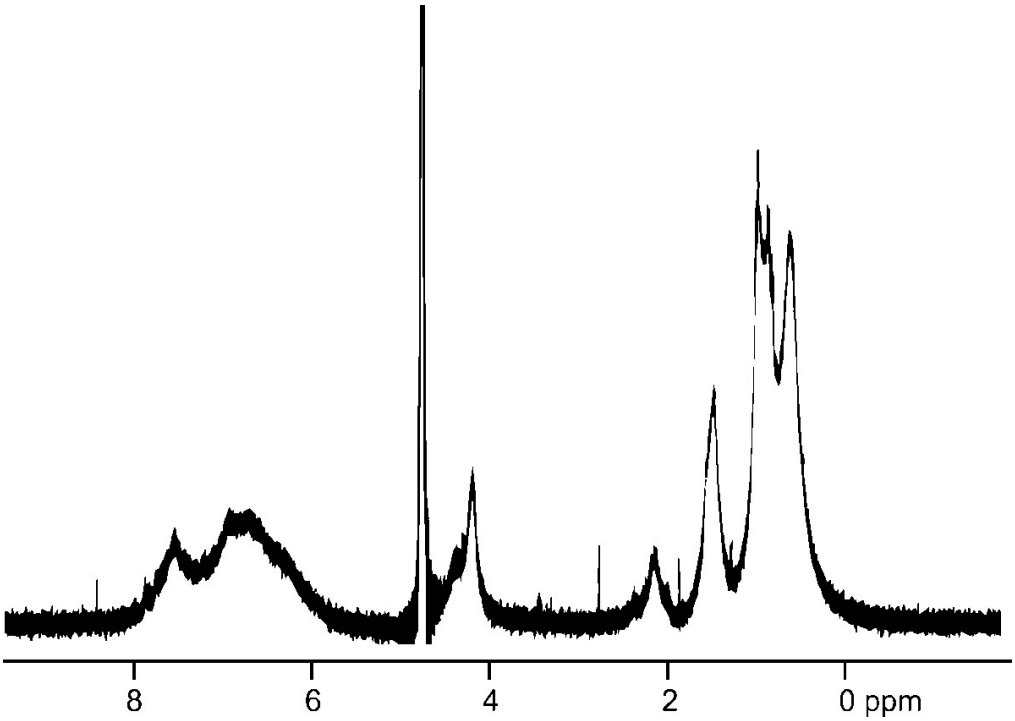

Figure S38. ^{1}H NMR spectrum of **1** at 5 mg/mL in D_2O at high pD showing broad resonances of compound. The T_1 and T_2 relaxation times were measured as 1.6 s and 9 ms for the aromatic protons and 0.66 s and 16 ms for the aliphatic protons respectively. The spectrum shown was recorded with a 30^{o} pulse, 16 scans and a signal acquisition time of 4 seconds. No apodisation was applied prior to Fourier transformation. The broadening around the base of the HDO peak at 4.7 ppm is due to truncation of the FID. T_2 values were measured using the CPMG sequence with the delay between the π pulses set at 2 ms and the number of pulses varied from 2 to 256 in 32 steps. T_1 values were measured using the inversion-recovery sequence with the inversion recovery time varied between 1 ms and 6 s in 16 steps.

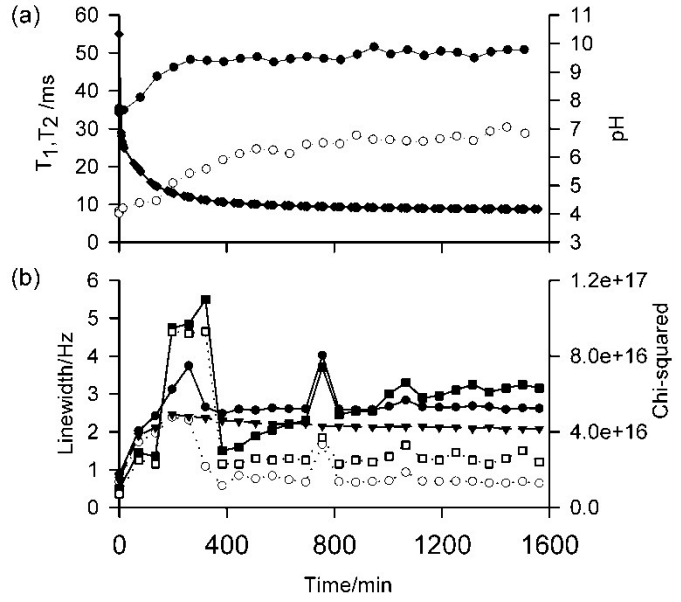

Figure S39. (a) Plots of $^{23}Na^+$ T_1 (black circle) and T_2 (white) relaxation times as a function of time following the addition of 4 mg/mL GdL to a solution of **2** at pH 10, along with pH measurements (black diamond). The lines are there to guide the eye. (b) Plot of fitted ^2H linewidths of dioxane-d_8 as a function of time: single Lorentzian fit (black triangle), wider component of double Lorentzian fit (black circle) and narrow component (white circle). Quality of fits are indicated by their chi-squared values (smaller value represents better fit): single component fit (black square) and double component (white square). Linewidths are the width of the fitted Lorentzian peaks at half height. (a) and (b) were acquired on the same sample. The time points at t = 0 were recorded prior to the addition of GdL.

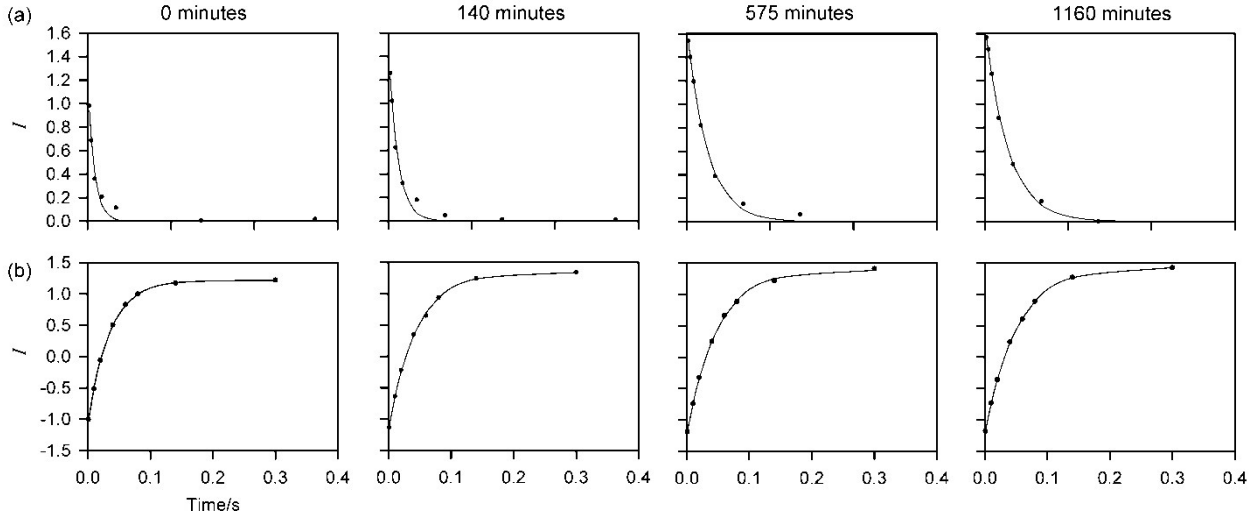

Figure S40. Example T_2 (a) and T_1 (b) $^{23}Na^+$ relaxation curves at times indicated since the addition of 4 mg/mL GdL to a solution of **2** at pH 10. Fits to equations S1 (T_1) and S2 (T_2) are shown as solid lines. Extracted T_1 and T_2 relaxation times are shown on Figure S39. Unlike **1**, the ^{23}Na CPMG relaxation curves (a) show clear deviation from monoexponential behaviour at early time points (plots at 0 and 140 minutes shown above). This implies that the structures present may be larger and/or more negatively charged than the structures formed by **1** and so the mobility of the $^{23}Na^+$ ions is restricted to a greater extent.[S6] Owing to time limitations during the experiment, only eight data points could be recorded for each decay curve and so fitting the data to biexponential functions would not be appropriate due to the inherent noise present in the data.

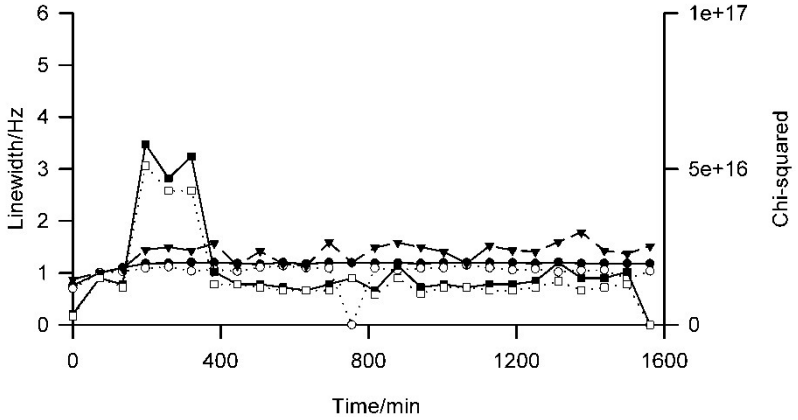

Figure S41. Plot of fitted ^{2}H linewidths of HDO as a function of time since addition of 4 mg/mL GdL to a solution of **2** at pH 10: single Lorentzian fit (black triangle), wider component of double Lorentzian fit (black circle) and narrow component (white circle). Quality of fits are indicated by their chi-squared values (smaller value represents better fit): single component fit (black square) and double component (white square).

4. Small angle neutron scattering

Solutions were prepared as described, with the H_2O and NaOH replaced with D_2O and NaOD. UV spectrophotometer grade, quartz cuvettes (Starna) with a 5 mm path length were filled with the solutions and for the gel samples this was immediately after the GdL was added and housed in a temperature controlled sample rack at 25±0.5 ºC during the gelation and measurements. Small angle neutron scattering (SANS) measurements of the gel**s** were performed using the SANS2D instrument (STFC ISIS Pulsed Neutron Source, Oxfordshire, UK). For the solutions the LOQ instrument at the same facility was used. On SANS2D a simultaneous Q-range [$Q = 4\pi sin(\theta/2)/\lambda$] of 0.006 to 0.7 $Å^{-1}$ was achieved utilizing an incident wavelength range of 1.75 to 16.5 Å and employing an instrument set up of L1=L2=4m, with the $1m^2$ detector offset vertically 60mm and sideways 100mm. Experimental measuring times were ~30 minutes. On LOQ A white beam of radiation with neutron wavelengths spanning 2.2 to 10 Å was used to access a Q range of 0.009 to ≥ 0.2 $Å^{-1}$ (at 25 Hz), with a fixed sample to main detector distance of 4.1 m. Experimental measuring times were ~60 minutes.

Scattering data from SANS2D and LOQ were (a) normalized for the sample transmission, (b) background corrected using a quartz cell, of the same path length, filled with D_2O (this also removes the inherent instrumental background arising from vacuum windows etc.) and (c) corrected for the linearity and efficiency of the detector response using the Mantid framework.[S7,S8] The data were put onto an absolute scale by reference to the scattering from a partially deuterated polystyrene blend.[S9] The instrument-independent data were then fitted to a customised model in the SasView software package[S10] primarily combining an absolute power law and a (Kratky-Porod) flexible cylinder,[S11,S12] as used previously.[S13] The Q-dependent power law (Q^{-N}) accounts for the mass fractal contribution to the scattering intensity which is superimposed on that from the fibrils. The fibrils themselves are represented as a flexible worm-like chain of cylindrical Kuhn segments. More details on the specific models used are given below.

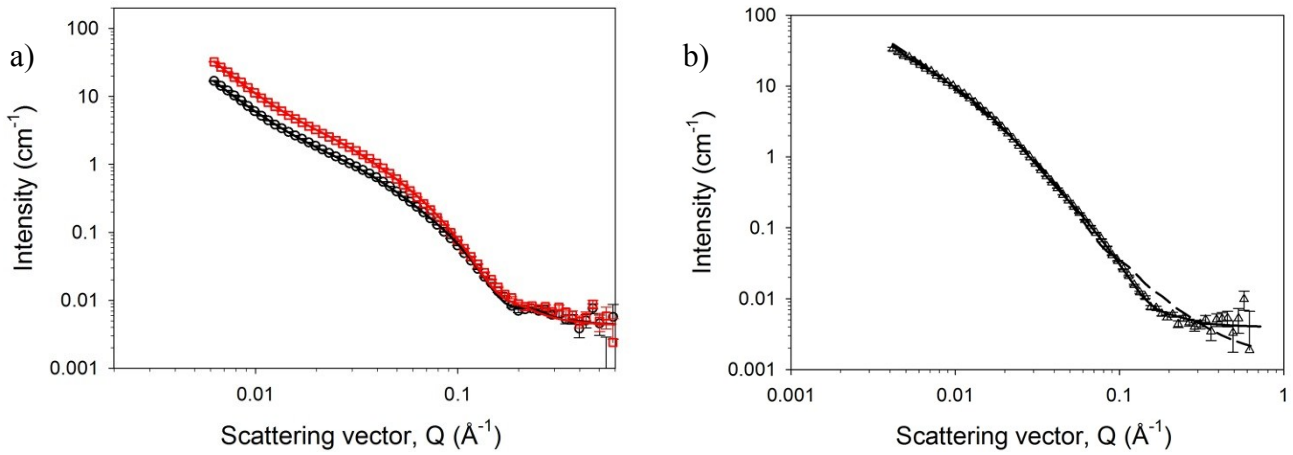

Figure S42. (a) SANS curves for the gel of **1** (black circles) and syneresed gel of **1** (red squares) and (b) the SANS data for the gel of **2** (black triangles). In all cases the best model fits are given as solid lines. For gel **1** using the flexible cylinder model with a circular cross-section combined with a power law available as a customized model within SasView.[S10] For gel **2** in (b) the dashed line represents the unsuccessful flexible cylinder model with a circular cross-section and the solid line is the flexible cylinder model with an elliptical cross-section combined with a power law available as a customized model within SasView.[S10]

	Gel of 1	**Syneresed gel of 1**	**Gel of 2** (unsuccessful fit)
Power law scale, SF_{PL} (/10^{-5})	6.2±0.2	3.8±0.8	26±20
Power law value, N	2.4±0.1	2.7±0.1	2.1±0.3
Cylinder scale, SF_{KP} (/10^{-3})	1.5±0.1	2.1±0.3	0.4±0.4
Radius, R (nm)	2.1±0.2	2.1±0.2*	4±2
Kuhn length, b (nm)	6.5±0.5	5.0±0.5	10±4
Contour length, L (nm)	25±2	36±3	240±50
Background (cm^{-1})	0.004±0.001	0.004±0.001	0.002±0.002

Table S1. The model fit parameters generated by fitting the customised flexible cylinder with a circular cross-section model to the data in SasView. Uncertainties were estimated as mentioned above. *This radius required a polydispersity of 0.2±0.1 in order to obtain a representative fit.

	Gel of 2
Power law scale, SF_{PL} ($/10^{-5}$)	3±1
Power law value, N	2.5±0.2
Cylinder scale, SF_{KP} ($/10^{-3}$)	0.22±0.02
Radius, R_{minor} (nm)	2.0±0.1
Radius axis ratio	5.1±0.5
Kuhn length, b (nm)	16±4
Contour length, L (nm)	90±20
Background (cm^{-1})	0.004±0.002

Table S2. The model fit parameters generated by fitting the customised flexible cylinder with an elliptical cross-section model to successfully fit the data for gel **2** in SasView. Uncertainties were estimated as mentioned above.

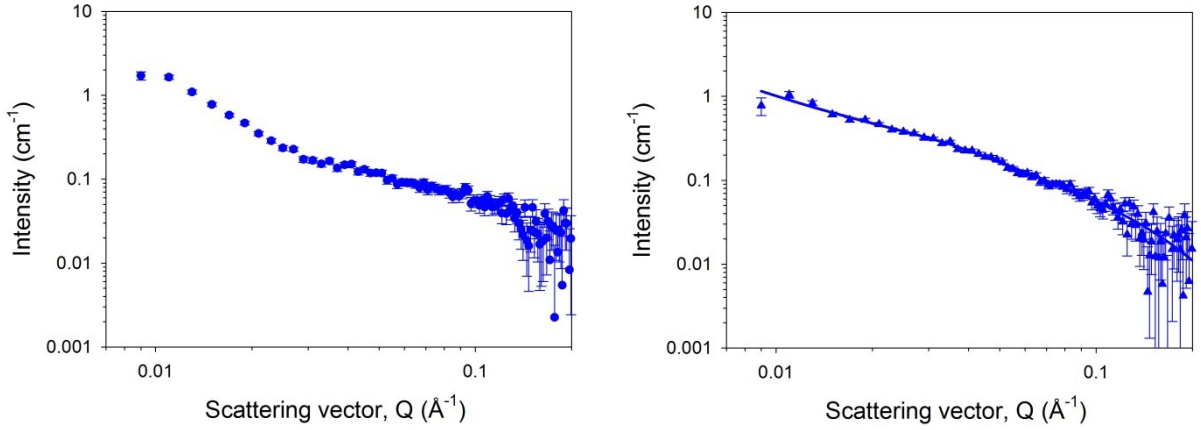

Figure S43. SANS data for the solution of (a) **1** (blue circles) and (b) **2** (blue triangles). For solution **1** in (a) the data is clearly inconsistent with the flexible cylinder model. The solution of **2** in (b) was successfully fitted using the flexible cylinder model with a circular cross-section combined with a power law, available as a customized model within SasView.[S10]

	Solution of 2
Power law scale (/10^{-5})	0.9±0.8
Power law value, N	2±1
Cylinder scale (/10^{-3})	2±1
Radius, R (nm)	1.2±0.7
Kuhn length (nm)	9±3
Length, L (nm)	20±10
Background (cm^{-1})	0.01±0.01

Table S3. The model fit parameters generated by fitting the customised flexible cylinder with a circular cross-section model to the data for the solution of **2** at 5 mg/mL solution at high pH, in SasView. Uncertainties were estimated as mentioned above.

SANS model fitting

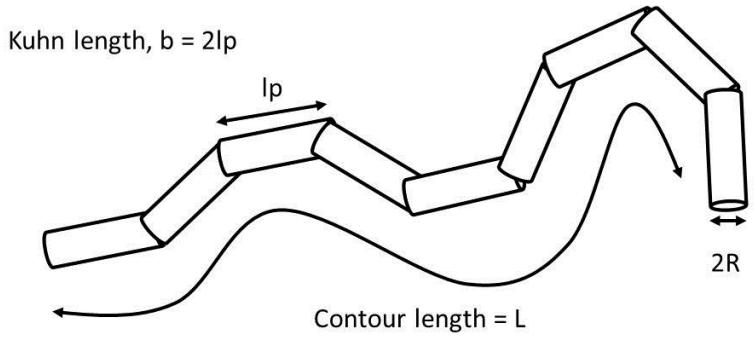

Figure S44. Schematic showing the parameters associated with the dimensions of the worm-like chain in the Kratky-Porod flexible cylinder model within SasView.[S10]

The model used to fit the SANS data was the Kratky-Porod (KP) flexible cylinder model combined with a power law,[S11,S12] which we have previously used and discussed in more detail.[S13] Here we will give a brief description. The flexible cylinder model describes a worm-like chain of contour length, L, made from freely jointed units with a segment length, lp, which is half of the Kuhn length fitting parameter, b, and a cross-sectional radius, R (Figure S44). The other parameters in the model include: an overall scale factor, SF_O, fixed at 1; a

simple numerical scaling factor for the power law component of the model, $SF_{PL,}$ related to the density of the network; a scale factor for the worm-like chain, SF_{KP}, corresponding to the volume fraction of the cylinders (of the size described by the model); a flat background to account for the incoherent background scattering from the sample; and, in some cases, a polydispersity parameter is also included, this applies a Gaussian distribution to the cross-sectional radius of the of the cylinder. The cylinder can have either a circular or an elliptical cross-section. For the elliptical cross-section the radius of the minor axis, R_{minor} is used as a parameter and the radius axis ratio is defined as R_{max}/R_{minor} and therefore will always be greater than 1.

When fitting, some conditions were imposed such as the Kuhn length had to be larger than 2R, and less than the overall length. The scattering length densities (SLDs) of the cylinder, made from gelator **1** ($1.5 \pm 0.5 \times 10^{-6}$ Å^{-2}) and gelator **2** ($1.6 \pm 0.5 \times 10^{-6}$ Å^{-2}), and the solvent, predominantly D_2O (6.3×10^{-6} Å^{-2}), were fixed. The slightly higher than theoretical value for the cylinder, of for example **1** (1.31×10^{-6} Å^{-2} for a bulk density of 1 g cm^{-3}) is to account for some hydration. This value is correlated with the SF_W parameter, but was kept constant in all fits and therefore does not impact on comparison of SF_W values between the two data sets relating to **1**. Certain parameters, which had a tendency towards unphysical values when allowed to be freely fitted, were iterated through in a stepwise manner and the values chosen when the fit was good, both visually and based on the minimum in χ^2. Uncertainties were taken based on where the fit began to deviate from a visually good quality fit.

5. References

S1. G. S. Vadehra, B. D. Wall, S. R. Diegelmann and J. D. Tovar, *Chem. Commun.*, 2010, **46**, 3947-3949.
S2. B. Botta, I. D'Acquarica, G. Delle Monache, D. Subissati, G. Uccello-Barretta, M. Mastrini, S. Nazzi and M. Speranza, *J. Org. Chem.*, 2007, **72**, 9283-9290.
S3. P. Rzepecki and T. Schrader, *J. Am. Chem. Soc.*, 2005, **127**, 3016-3025.
S4. J. Raeburn, L. Chen, S. Awhida, R. C. Deller, M. Vatish, M. I. Gibson and D. J. Adams, *Soft Matter*, 2015, **11**, 3706-3713.
S5. M. Wallace, J. A. Iggo and D. J. Adams, *Soft Matter*, 2015, **11**, 7739-7747.
S6. W. H. Braunlin, H. J. Vogel and S. ForsÉN, *Eur. J. Biochem.*, 1984, **142**, 139-144.
S7. O. Arnold, J. C. Bilheux, J. M. Borreguero, A. Buts, S. I. Campbell, L. Chapon, M. Doucet, N. Draper, R. Ferraz Leal, M. A. Gigg, V. E. Lynch, A. Markvardsen, D. J. Mikkelson, R. L. Mikkelson, R. Miller, K. Palmen, P. Parker, G. Passos, T. G. Perring, P. F. Peterson, S. Ren, M. A. Reuter, A. T. Savici, J. W. Taylor, R. J. Taylor, R. Tolchenov, W. Zhou and J. Zikovsky, *Nuclear Instruments and Methods in Physics Research Section A: Accelerators, Spectrometers, Detectors and Associated Equipment*, 2014, **764**, 156-166.
S8. https://www.mantidproject.org.
S9. G. D. Wignall and F. S. Bates, *J. Appl. Crystallogr.*, 1987, **20**, 28-40.
S10. https://www.sasview.org.
S11. J. S. Pedersen and P. Schurtenberger, *Macromolecules*, 1996, **29**, 7602-7612.
S12. W.-R. Chen, P. D. Butler and L. J. Magid, *Langmuir*, 2006, **22**, 6539-6548.
S13. E. R. Draper, L. L. E. Mears, A. M. Castilla, S. M. King, T. O. McDonald, R. Akhtar and D. J. Adams, *RSC Advances*, 2015, **5**, 95369-95378.